Prodrugs of pyrazolo[3,4-d]pyrimidines: from library synthesis to evaluation as potential anticancer agents in an orthotopic glioblastoma model

Journal of Medicinal Chemistry

Article

Prodrugs of pyrazolo[3,4-*d*]pyrimidines: from library synthesis to evaluation as potential anticancer agents in an orthotopic glioblastoma model

Giulia Vignaroli, Giulia Iovenitti, Claudio Zamperini, Federica Coniglio, Pierpaolo Calandro, Alessio Molinari, Anna Lucia Fallacara, Andrea Sartucci, Alessia Calgani, David Colecchia, Andrea Mancini, Claudio Festuccia, elena dreassi, Massimo Valoti, Francesca Musumeci, Mario Chiariello, Adriano Angelucci, Maurizio Botta, and Silvia Schenone

J. Med. Chem., **Just Accepted Manuscript** • DOI: 10.1021/acs.jmedchem.7b00637 • Publication Date (Web): 26 Jun 2017

Just Accepted

ACS Publications

Journal of Medicinal Chemistry is published by the American Chemical Society. 1155 Sixteenth Street N.W., Washington, DC 20036

PRODRUGS OF PYRAZOLO[3,4-*d*]PYRIMIDINES: FROM LIBRARY SYNTHESIS TO EVALUATION AS POTENTIAL ANTICANCER AGENTS IN AN ORTHOTOPIC GLIOBLASTOMA MODEL

Giulia Vignaroli,[†,‖] Giulia Iovenitti,[†,‖] Claudio Zamperini,[†,‖] Federica Coniglio,[†,‖] Pierpaolo Calandro,[†] Alessio Molinari,[†] Anna Lucia Fallacara,[†] Andrea Sartucci,[†] Alessia Calgani,[‡] David Colecchia,[¥] Andrea Mancini,[‡] Claudio Festuccia,[‡] Elena Dreassi,[†] Massimo Valoti,[§] Francesca Musumeci,[ꞁ] Mario Chiariello,[¥] Adriano Angelucci,[‡] Maurizio Botta,*[†,‖,·] Silvia Schenone[¥]

[†]Dipartimento di Biotecnologie, Chimica e Farmacia, Università degli Studi di Siena, Via Aldo Moro 2, 53100 Siena, Italy; [‖]Lead Discovery Siena S.r.l., via Vittorio Alfieri 31, 53019, Castelnuovo Berardenga, Siena (IT); [‡]Dipartimento di Scienze Cliniche Applicate e Biotecnologiche, Università dell'Aquila, Via Vetoio, 67100 Coppito, L'Aquila, Italy; [¥]Consiglio Nazionale delle Ricerche, Istituto di Fisiologia Clinica and Istituto Toscano Tumori, Core Research Laboratory, Via Fiorentina 1, 53100, Siena (IT); [§] Dipartimento di Scienze della Vita, Università degli Studi di Siena, Via Aldo Moro 2, 53100 Siena, Italy; [ꞁ]Dipartimento di Scienze Farmaceutiche, Università degli Studi di Genova, Viale Benedetto XV 3, 16132 Genova, Italy; [·] Sbarro Institute for Cancer Research and Molecular Medicine, Center for Biotechnology, College of Science and Technology, Temple University, BioLife Science Building, Suite 333, 1900 N 12th Street, Philadelphia, Pennsylvania 19122.

ABSTRACT

Pyrazolo[3,4-*d*]pyrimidines are potent protein kinase inhibitors with promising antitumor activity but suboptimal aqueous solubility, consequently worth to be further optimized. Herein, we present the one-pot two-step procedure for the synthesis of a set of pyrazolo[3,4-*d*]pyrimidine prodrugs (**1a-9a,e**) with higher aqueous solubility and enhanced pharmacokinetic and therapeutic properties. ADME studies demonstrated for the most promising prodrugs a better aqueous solubility, a favorable hydrolysis in human and murine serum and an increased ability to cross cell membranes with respect to the parental drugs, explaining their better 24h *in vitro* cytotoxicity against human glioblastoma U87 cell line. Finally, the **4-4a** couple of drug/prodrug was also evaluated *in vivo*, revealing a profitable pharmacokinetic profile of the prodrug associated with a good efficacy. The application of the prodrug approach demonstrated to be a successful strategy for improving aqueous solubility of the parental drugs determining a positive impact also in their biological efficacy.

INTRODUCTION

During the last years, several pyrazolo[3,4-*d*]pyrimidine derivatives have been studied and synthesized by our research group. To date, our pyrazolo[3,4-*d*]pyrimidine library consists of more than 400 members, developed mostly as ATP-competitive tyrosine kinase inhibitors.[1] The SRC kinases are key molecular targets in cancer therapy; their family includes the nine non-receptor tyrosine kinases Src, Yes, Fyn, Hck, Lyn, Blk, Fgr, Lck and Frk. These kinases are activated or overexpressed in many cancer types and are involved in the regulation of cell proliferation, survival, invasion and angiogenesis, thus playing a crucial role in tumor development and progression.[2]

The anticancer activity of pyrazolo[3,4-*d*]pyrimidines was confirmed in several cancer cell lines, both from solid tumors (i.e. osteosarcoma SaOS-2,[3] prostate PC3,[4] neuroblastoma SH-SY5Y,[5-6] glioblastoma U87,[7-8] rhabdomyosarcoma[9], mesothelioma[10], medulloblastoma[11], medullary thyroid carcinoma[12]) and leukemia (i.e. 32D-p210 and 32D-T315I) [13] and Burkitt lymphomas.[14] *In vivo* data, generated in subcutaneous xenograft mouse models further supported the antitumor activities of several pyrazolo[3,4-*d*]pyrimidines against leukemia (32D-p210 and 32D-T315I),[13] neuroblastoma (SH-SY5Y),[5] and glioblastoma (U87).[8] With regards to glioblastoma (GBM), targeting of the activated Src might play an important role in reducing the high proliferation and invasion capacity that characterizes this tumor. GBM is the most frequent primary brain tumor in adults and still poses clinical challenges since the available therapeutic choices, including surgical resection, followed by concomitant radiotherapy and temozolomide therapy, do not significantly improve the prognosis.[15] Targeted therapy might offer new opportunities, but to date it is facing two important issues: the selection of the most adequate molecular target and the low drug delivery to the brain.[16] In our recent study, a selected pyrazolo[3,4-*d*]pyrimidine was able to increase the survival time of treated mice in a GBM (U87 cells) orthotopic model by 30%, with respect to the vehicle-

treated mice.[8] Despite their promising biological activity, pyrazolo[3,4-*d*]pyrimidines have low aqueous solubility, a property that could interfere with the development of these compounds to become drug candidates.[17-18] In this context, early assessment of pharmaceutical properties such as solubility, metabolic stability and permeability has become a key step in the drug discovery process,[19] as it is estimated that around 40% of potential drug candidates fail to reach the market due to poor physicochemical properties.[20-21] Accordingly, the development of potential alternative strategies to improve properties like solubility, tissue distribution, efficacy and toxicity should be considered in the very early stages of preclinical development.

In this view, together with the optimization of the biological activity of these compounds we are studying several strategies to improve their aqueous solubility and pharmacokinetic properties (i.e. prodrugs,[22] cyclodextrins,[17] albumin nanoparticles,[23] liposomes [23]).

As for the prodrug approach,[24-25] we recently reported that (I) the secondary amino group at C4 of the pyrazolo[3,4-*d*]pyrimidine nucleus was the most suitable position to connect with the prodrug moiety, (II) the *N*-methylpiperazino group was effective in increasing the water solubility of the resulting prodrugs in comparison to the parent drugs and, (III) the *O*-alkyl carbamate was a suitable *in vivo*-hydrolysable linker to connect the secondary amino group at C4 with the solubilizing entity.[22]

Based on these data, in the current study we advanced the development of pyrazolo[3,4-*d*]pyrimidine prodrugs as a valid approach to overcome the low water solubility of this class of compounds. The study started with the optimization of the previously reported chemical synthesis. The resulting one-pot, two-step procedure was efficiently applied to nine selected pyrazolo[3,4-*d*]pyrimidine parent drugs (**1-9**) presenting different chemical moieties.[5,13,26-29] To further demonstrate the versatility of the chemical approach, a series of prodrugs (**9a-9e**) with increased steric bulk on the prodrug moiety was synthesized. All the synthesized compounds were

characterized for their water solubility, stability in polar media, apparent permeability (PAMPA) as well as metabolic stability (with Human Liver Microsomes, HLM) and plasma hydrolysis.

Then the most interesting prodrugs were tested in a cellular assay with human GBM U87 cell line to assess their biological activity as well as the kinetics of uptake and hydrolysis in a cellular setting. As *in vivo* proof of concept, the pharmacokinetics of the most promising pair of drug and prodrug were studied, followed by the analysis of their pharmacological activities in an orthotopic mouse model of GBM.

RESULTS

Synthesis

One aim of this study was to define the most versatile chemical approach for the synthesis of prodrugs starting from different pyrazolo[3,4-*d*]pyrimidines. The synthesis of prodrugs (**1a-8a** and **9a-e**) was performed applying a one-pot, two-step procedure, starting from the appropriate drug (**1-9**),[5,13,26-29] which by reaction with trisphosgene generated the carbonyl-chloride intermediate on the secondary amine at C4. The displacement of the chlorine using the appropriate alcohol afforded the final products **1a-8a** and **9a-e**, with overall yields ranging from 25 to 85% (Scheme 1 and 2).

Scheme 1. Synthesis of Prodrugs 1a-8a[a]

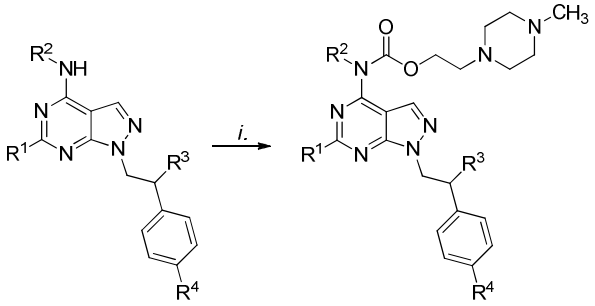

1, 1a: R^1 = H; R^2 = $CH_2C_6H_5$; R^3 = Cl; R^4 = H
2, 2a: R^1 = H; R^2 = $CH_2C_6H_4$*o*Cl; R^3 = Cl; R^4 = Br
3, 3a: R^1 = SCH_3; R^2 = C_6H_4*m*Cl; R^3 = H; R^4 = H
4, 4a: R^1 = $SCH_2CH_2$4-morpholin; R^2 = C_6H_4*m*Br; R^3 = Cl; R^4 = H
5, 5a: R^1 = SCH_3; R^2 = $CH_2CH_2C_6H_5$; R^3 = Cl; R^4 = H
6, 6a: R^1 = H; R^2 = C_6H_5; R^3 = Cl; R^4 = Br
7, 7a: R^1 = SCH_3; R^2 = C_6H_4*m*Cl; R^3 = Cl; R^4 = H
8, 8a: R^1 = SCH_2CH_3; R^2 = *n*Bu; R^3 = Cl; R^4 = H

[a]Reagents and Conditions: *i.* triphosgene, $NaHCO_3$, DCM; 3 h, 0 °C to r.t., then 2-(4-methylpiperazin-1-yl)ethanol (**12**) in DCM, r.t. 16 h.

For compounds **1a-8a** the appropriate derivative was reacted with 2-(4-methylpiperazin-1-yl)ethanol (**12**). Alcohol **12** was prepared by nucleophilic substitution of the bromine of 1-bromo-2-ethanol (**10**) with *N*-methylpiperazine (Scheme 3, A). Compounds **1-8** were dissolved in DCM and reacted with triphosgene in the presence of an excess of sodium bicarbonate. The reaction was monitored by TLC and as soon as the starting material disappeared, a solution of the alcohol **12** in DCM was added. The reaction mixture was then stirred at room temperature overnight. Prodrugs **9a-9e** were prepared starting from compound **9**, applying the same synthetic approach but using different alcohols (**12**, **13** and **17-19**) (Scheme 2). Prodrugs **9a-9e** were synthesized in order to have a series of derivatives with increasing steric hindrance close to the carbamate prodrug moiety. Prodrugs **9a-9e** show H, Me, Et, Ph and Bn at the C1 position of the prodrug moiety.

Scheme 2. Synthesis of Prodrugs 9a-e[a]

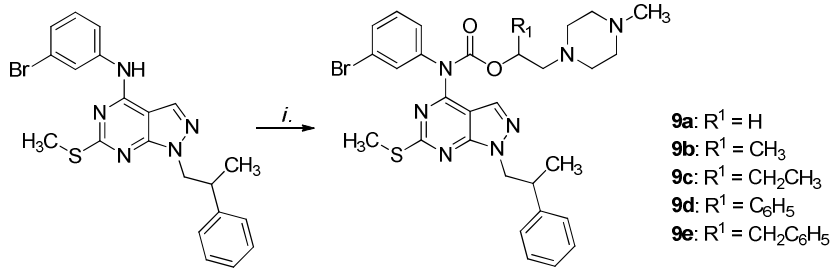

9 **9a-9e**

[a]Reagents and Conditions: *i.* triphosgene, $NaHCO_3$, DCM; 3 h, 0 °C to r.t., then 2-(4-methylpiperazin-1-yl)CH_2CHR^1OH (R^1=H, **12** or R^1=CH_3, **13** or R^1=CH_2CH_3, **17** or R^1=C_6H_5, **18** or R^1=$CH_2C_6H_5$, **19**) in DCM, r.t. 16 h.

Alcohol **13** was synthesized similarly to compound **12** starting from 1-bromo-2-propanol (**11**), whereas alcohols **17** and **18** were prepared from reaction of *N*-methylpiperazine with different epoxides, 1,2-epoxybutane (**14**) and styrene oxide (**15**), respectively.[30,31] Lastly, compound **19** was synthesized starting from 2-benzyloxirane (**15**) using zinc chloride and *N*-methylpiperazine.

Scheme 3. Synthesis of Alcohols 12,13 and 17-19[a]

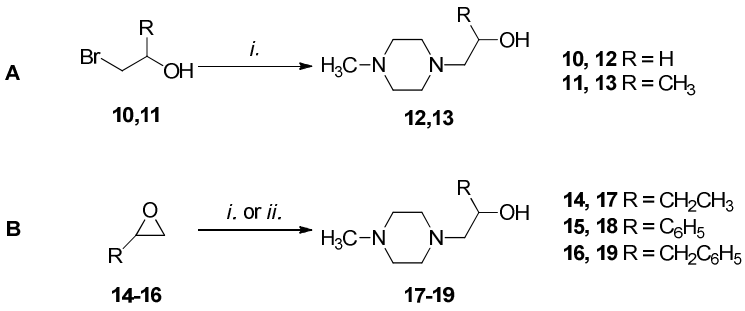

[a]Reagents and Conditions: for compounds **12,13** and **17,18** *i*. *N*-methylpiperazine, K_2CO_3, toluene, 12 h; for compound **19** *ii.* *N*-methylpiperazine, $ZnCl_2$, ACN_{dry}, reflux, 12 h

The synthetic approach here reported was suitable for pyrazolo[3,4-*d*]pyrimidines bearing different chemical features. For instance, the C4 position, which is directly involved in the prodrug-carbamate formation, presented alkyl (**8**), phenyl (**3**, **6**, **7** and **9**), benzyl (**1** and **2**) as well as phenylethyl groups (**5**). In the previously reported synthetic approach triphosgene and sodium

bicarbonate were used to form the carbamic-chloride intermediate that, after isolation, was reacted with 2-(4-methylpiperazin-1-yl)ethanol (**12**) using sodium hydride as base.[22] The new strategy is carried out as a one-pot, two-step procedure, using sodium bicarbonate as the only base. In this way, the time consuming and delicate isolation of the unstable carbamic-chloride intermediate is avoided, with an increase of the resulting yields. In fact, the synthesis of **9a** by the first approach resulted in a yield of 18%, whereas the new synthesis produced a 30% yield of the final prodrug.

***In vitro* ADME**

Several *in vitro* assays were performed to evaluate the ADME properties of the synthesized prodrugs (**1a-8a** and **9a-9e**) and to compare them to their parent drugs (**1-9**). Initially, the stability in several media [phosphate saline buffer (PBS), methanol (MeOH) and human plasma (Plasma)] was studied (Table 1). Next, the aqueous solubility and the apparent permeability (PAMPA) towards gastrointestinal membrane (GI) and blood brain barrier (BBB) were investigated, as well as the stability in the presence of human liver microsomes (HLM) (Table 2).

Table 1. Stability of prodrugs 1a-8a, 9a-9e in phosphate saline buffer (PBS), methanol (MeOH) and human plasma (Plasma)[a]

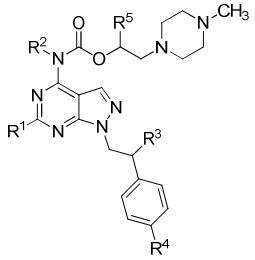

Cpd	R^1	R^2	R^3	R^4	R^5	PBS $t_{1/2}$ (h)	MeOH $t_{1/2}$ (h)	Plasma $t_{1/2}$ (h)
1a	H	$CH_2C_6H_5$	Cl	H	H	>48	>48	64.4
2a	H	$CH_2C_6H_4o$Cl	Cl	Br	H	>48	>48	75.0
3a	SCH_3	C_6H_4mCl	H	H	H	>48	>48	3.13
4a	$SCH_2CH_2$4-morpholino	C_6H_4mBr	Cl	H	H	>48	>48	3.48
5a	SCH_3	$CH_2CH_2C_6H_5$	Cl	H	H	>48	>48	45.2

6a	H	C_6H_5	Cl	Br	H	>48	>48	5.68
7a	SCH_3	C_6H_4*m*Cl	Cl	H	H	>48	>48	3.71
8a	SCH_2CH_3	*n*Bu	Cl	H	H	1.0	2.0	0.46
9a	SCH_3	C_6H_4*m*Br	CH_3	H	H	>48	>48	3.21
9b	SCH_3	C_6H_4*m*Br	CH_3	H	CH_3	>48	>48	10.4
9c	SCH_3	C_6H_4*m*Br	CH_3	H	CH_2CH_3	>48	>48	11.3
9d	SCH_3	C_6H_4*m*Br	CH_3	H	C_6H_5	<0.25	<0.25	ND[b]
9e	SCH_3	C_6H_4*m*Br	CH_3	H	$CH_2C_6H_5$	>48	>48	40.0

[a]Determined by UV/LC-MS, $t_{1/2} = ln\ 2/K_{obs}$. Concentration of each compound 100 μM. [b]Not Determined.

Stability in polar media such as methanol and PBS was analysed by UV/LC-MS, after dissolving the compound in the appropriate media. Resulting half-lives were greater than 48 h for prodrugs **1a-7a**, **9a-c** and **9e** (Table 1). These values indicated the good stability of these compounds, which were thus regarded as chemically stable for the subsequent studies. On the other hand, prodrugs **8a**[17] and **9d**, showed low stability in the polar media tested (Table 1). This high rate of hydrolysis is the reason why these compounds could not be tested for their aqueous solubility, the ability to overcome membranes as well as their metabolic stability. For **9d**, even the plasma hydrolysis could not be analysed as it demonstrated a half-life less than 15 min in PBS and methanol.

A key property to be evaluated was the rate of plasma hydrolysis. In fact, our prodrugs display an *O*-alkyl-carbamate linker that should undergo *in vivo* hydrolysis in order to release the active compound. Prodrugs **1a-8a** and **9a-9e** were incubated in human plasma at 37 °C, and their disappearance, together with the formation of the respective drugs **1-9**, was monitored by UV/LC-MS (Table 1). Prodrugs with a plasma half-life higher than 40 h were **1a** ($t_{1/2}$ = 64.4 h), **2a** ($t_{1/2}$ = 75.0 h), **5a** ($t_{1/2}$ = 45.2 h) and **9e** ($t_{1/2}$ = 40.0 h). These compounds (**1a**, **2a**, **5a** and **9e**) present a common chemical feature: a phenyl ring spaced by one or two methylene groups from the carbamate group. In fact, prodrugs **1a**, **2a** and **5a** show a benzyl or phenethyl amine in the C4 position of the pyrazolo[3,4-*d*]pyrimidine nucleus, whereas prodrug **9e** has a benzyl group at the

C1 position of the *O*-alkyl-carbamate prodrug moiety. Prodrugs **9b** and **9c**, with a methyl and ethyl group at the C1 position of the *O*-alkyl-carbamate moiety, showed half-lives of 10.4 h and 11.3 h, respectively, whereas compounds **3a**, **4a**, **6a**, **7a** and **9a**[22] displayed plasma half-lives lower than 6 h ($t_{1/2}$ of 3.13 h, 3.48 h, 5.68 h, 3.71 h and 3.21 h, respectively). Also these compounds (**3a**, **4a**, **6a**, **7a** and **9a**) share a common chemical feature: a substituted aniline in the C4 position and a basic *O*-alkyl-carbamate group. For compound **8a**, the plasma half-life confirmed the data obtained by stability assays, highlighting that the contribution of solvent-mediated hydrolysis in the cleavage of this prodrug cannot be ignored. Subsequently, the passive membrane permeability was evaluated performing two different PAMPA assays, one reproducing the GI membrane, the other the BBB (Table 2). Prodrugs **1a**, **2a**, **4a** and **5a** demonstrated an apparent permeability lower than their respective drug (**1**, **2**, **4** and **5**) towards GI membrane and BBB. On the contrary, compounds **3a**, **7a**, and **9a-c** and **9e** showed an improved ability of overcoming these artificial membranes. Pair **6-6a** exhibited a mixed behaviour with prodrug **6a** showing enhanced permeability towards GI membrane but minor towards BBB, in comparison with drug **6**. Prodrug **8a** and **9d**, as previously mentioned, could not be tested due to their limited stability in polar media. To study CYP-metabolism, compounds **1a, 4a** and **9a** were incubated for one hour at 37 °C with a solution of man-pooled HLM. After this time, the percentage of prodrugs and metabolites was determined by HPLC–MS analysis. The percentage of unmodified prodrug recovered after the incubation was 86.4% for compound **1a**, 93.6% for **4a** and 99.9% for **9a**, suggesting that these compounds are not a direct substrate of CYP enzymes (Table 2). The parent drugs were previously reported as metabolic stable (metabolic stability higher than 78.3%). Interestingly, the pattern of metabolites generated from prodrugs was similar to the one obtained from the respective drugs, results that further support the hypothesis that the prodrug linker is not a substrate of CYP-metabolism (see supporting information for further details).

Table 2. Apparent permeability, aqueous solubility and metabolic stability of parent compounds 1-9 and prodrugs 1a-8a, 9a-9e[a]

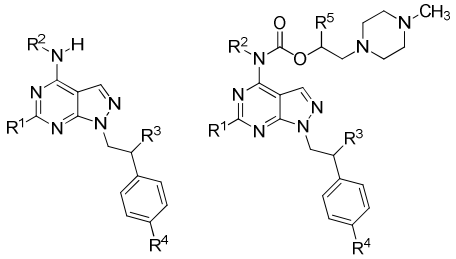

Cpd	R^1	R^2	R^3	R^4	R^5	GI[b] P_{app} (10^{-6} cm·sec^{-1})	BBB[c] P_{app} (10^{-6} cm·sec^{-1})	H_2O Sol. μg·mL^{-1}	Metabolic Stab.[d] %
1	H	$CH_2C_6H_5$	Cl	H	-	11.08	16.5	0.70	78.3
1a	H	$CH_2C_6H_5$	Cl	H	H	6.70	5.01	18.81	86.4
2	H	$CH_2C_6H_4o$Cl	Cl	Br	-	8.78	13.23	<0.01	95.2
2a	H	$CH_2C_6H_4o$Cl	Cl	Br	H	2.38	1.92	1.95	ND[e]
3	SCH_3	C_6H_4mCl	H	H	-	0.25	1.48	0.12	99.0
3a	SCH_3	C_6H_4mCl	H	H	H	4.69	4.30	6.32	ND[e]
4	$SCH_2CH_2$4-morpholino	C_6H_4mBr	Cl	H	-	5.27	7.10	3.70	97.2
4a	$SCH_2CH_2$4-morpholino	C_6H_4mBr	Cl	H	H	2.13	2.91	8.70	93.6
5	SCH_3	$CH_2CH_2C_6H_5$	Cl	H	-	7.40	6.17	0.07	96.2
5a	SCH_3	$CH_2CH_2C_6H_5$	Cl	H	H	0.85	0.01	106.97	ND[e]
6	H	C_6H_5	Cl	Br	-	6.64	13.10	0.06	96.4
6a	H	C_6H_5	Cl	Br	H	9.91	6.97	41.56	ND[e]
7	SCH_3	C_6H_4mCl	Cl	H	-	0.26	3.14	0.13	91.1
7a	SCH_3	C_6H_4mCl	Cl	H	H	4.95	4.14	4.22	ND[e]
8	SCH_2CH_3	*n*Bu	Cl	H	-	5.99	9.99	0.05	91.5
9	SCH_3	C_6H_4mBr	CH_3	H	-	0.01	0.50	0.01	95.1
9a	SCH_3	C_6H_4mBr	CH_3	H	H	2.11	1.89	6.47	99.9
9b	SCH_3	C_6H_4mBr	CH_3	H	CH_3	2.15	2.39	3.40	ND[e]
9c	SCH_3	C_6H_4mBr	CH_3	H	CH_2CH_3	1.45	0.93	1.96	ND[e]
9e	SCH_3	C_6H_4mBr	CH_3	H	$CH_2C_6H_5$	2.32	1.01	0.99	ND[e]

[a]Determined by UV/LC-MS See experimental section for details. [b]Gastro-Intestinal Parallel Artificial Membrane Permeability Assay. [c]Blood Brain Barrier Parallel Artificial Membrane Permeability Assay. [d]Expressed as percentage of unmodified drug. [e]Not Determined.

***In vitro* biological assays**

Parent drugs **1**, **4**, **6** and **9**, were previously reported and studied for their activity against c-Src and c-Abl. [5,13] Herein, a cell-free assay was performed to determine k_i values of selected prodrugs (**4a**, **9a**, **9b** and **9e**) and to monitor the potential inhibitory activity of these compounds before *in vivo* hydrolysis (see supporting info for method details). The results of the enzymatic assays showed that prodrugs were not able to inhibit directly c-Src and c-Abl at the concentrations tested (below 100 µM). These data support the hypothesis that prodrugs have a limited intrinsic inhibitory activity (Table 3).

Table 3. Biological data: enzymatic and cellular assays

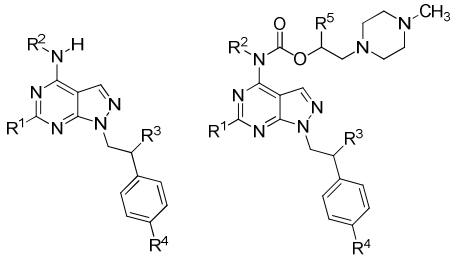

Cpd	R^1	R^2	R^3	R^4	R^5	Src (Ki µM)	Abl (Ki µM)	U87 IC_{50} µM 24h	U87 IC_{50} µM 48h	U87 IC_{50} µM 72h
1	H	$CH_2C_6H_5$	Cl	H	-	3.0	0.37	14.6 ± 1.3	4.9 ± 1.2	2.9 ± 1.1
1a	H	$CH_2C_6H_5$	Cl	H	H	ND[b]	ND[b]	18.6 ± 1.2	15.2 ± 1.1	15.0 ± 1.2
4	$SCH_2CH_2$4-morpholine	C_6H_4mBr	Cl	H	-	0.13	0.12	17.3 ± 1.7	6.8 ± 2.8	1.9 ± 1.2
4a	$SCH_2CH_2$4-morpholine	C_6H_4mBr	Cl	H	H	>100	>100	7.5 ± 1.4	5.2 ± 1.9	1.8 ± 1.8
6	H	C_6H_5	Cl	Br	-	0.06	0.61	25.3 ± 1.8	17.3 ± 1.9	14 ± 1.9
6a	H	C_6H_5	Cl	Br	H	ND[b]	ND[b]	8.2 ± 1.7	5.1 ± 1.5	2.0 ± 1.4
7	SCH_3	C_6H_4mCl	Cl	H	-	0.72	0.6	21.8 ± 1.9	17.2 ± 1.7	12.5 ± 1.7
7a	SCH_3	C_6H_4mCl	Cl	H	H	ND[b]	ND[b]	11.5 ± 1.2	7.9 ± 1.3	2.54 ± 1.3
9	SCH_3	C_6H_4mBr	CH_3	H	-	0.02	1.07	16.2 ± 1.2	2.3 ± 1.3	1.5 ± 1.1
9a	SCH_3	C_6H_4mBr	CH_3	H	H	>100	>100	7.3 ± 1.5	2.2 ± 1.1	1.57 ± 1.2
9b	SCH_3	C_6H_4mBr	CH_3	H	CH_3	>100	>100	7.4 ± 1.9	4.5 ± 1.7	1.8 ± 1.5
9c	SCH_3	C_6H_4mBr	CH_3	H	CH_2CH_3	ND[b]	ND[b]	7.7 ± 1.9	6.4 ± 1.4	2.0 ± 1.1
9e	SCH_3	C_6H_4mBr	CH_3	H	$CH_2C_6H_5$	>100	>100	6.7 ± 1.8	2.45 ± 1.3	1.69 ± 1.5

GBM U87 cell line. Cells were treated for 24 h, 48 h and 72h with different concentrations of compound (0.1 μM, 1 μM, 5 μM, 10 μM). [a]IC_{50}: the half maximal inhibitory concentration of the effectiveness in reducing the number of viable cells with respect to untreated cells. [b] Not determined.

Cellular assays were performed in the human GBM U87 cell line in order to characterize the cytotoxicity of the prodrugs and their parent active compounds. Cells were treated for 24, 48 and 72 h with increasing concentrations of the compounds (0.1 μM, 1 μM, 5 μM, 10 μM). IC_{50} values were calculated counting viable cells compared to untreated cells (Table 3). At 24 h, prodrugs with an *in vitro* plasma half-life lower than 41 h, namely **4a**, **9a**, **9b** and **9e**, showed an activity higher than their respective drug (Table 3).

At 48 h and 72 h, the same prodrugs (**4a**, **9a**, **9b** and **9e**) demonstrated an activity comparable to the one of their parent drugs (Table 3). On the contrary, prodrug **1a** was less active than drug **1** at 24, 48 and 72 h.

In most cases, prodrugs were more effective than the respective drug at 24 h, although they demonstrated an efficacy comparable to the parent compound at 48 h and 72 h. In order to understand if this effect may be related to an enhanced ability to enter into the cytoplasm, a cellular kinetics assay was performed (Fig. 1). GBM U87 cells were treated with prodrugs **4a**, **9a-b** and **9e** and drugs **4** and **9** at a concentration of 20 μM and the quantity of compound inside the cell was determined by HPLC.

A

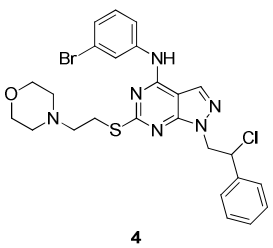

4

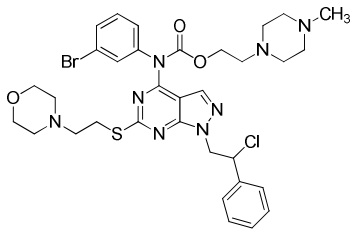

4a

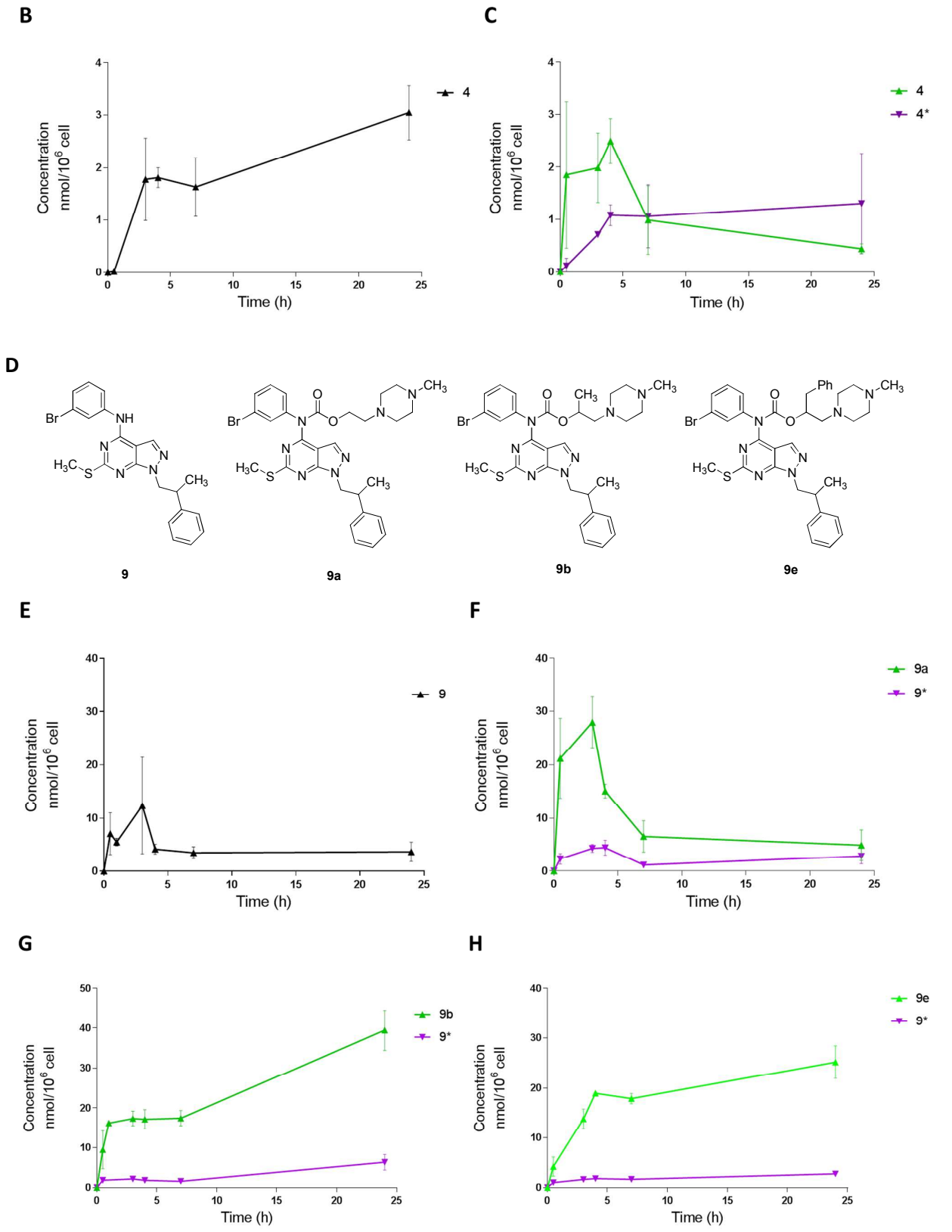

Figure 1. Cellular kinetics of drug/prodrug: 4/4a and 9/9a, 9b, 9e. A) Chemical structures of compound **4** and **4a**. B, C) Time-dependent concentration of drug and prodrugs within cells after treatment with compounds **4** (B) and prodrug **4a** (C). D) Chemical structures of compound **9**, **9a**, **9b** and **9e**. E, F, G, H) Time-dependent concentration of drug and prodrugs within cells after treatment with the following compounds: drug **9** (E),

prodrug **9a** (F), prodrug **9b** (G), prodrug **9e** (H).
The curves display the quantity of compound (nanomoles) found within the cells at several time points (0.5, 3.0, 4.0, 7.0, 24.0 h). For prodrugs (**4a** and **9a**, **9b**, **9e**) the green curve shows the quantity of prodrug whereas the purple line indicates quantity of drug released after hydrolysis (**4*** and **9***). Human GBM U87 cells were treated with drugs **4** and **9** and prodrugs **4a**, **9a**, **9b** and **9e** at a concentration of 20 μM for different time periods. Cells were lysed and the quantity of compound within the cytoplasm was determined by HPLC.

Compounds **4** and **9** were selected as representative of two opposite situations, as they are the most and the least hydrophilic drug of the set of pyrazolo[3,4-*d*]pyrimidines studied herein. Cellular kinetics showed that prodrugs were subjected to a faster uptake compared to the respective drugs. Moreover, the quantity of each prodrug within the cytoplasm was higher than the quantity of the corresponding drug. However, the amount of each drug released from its prodrug was comparable to the quantity of drug obtained after treatment with the free drug only. Interestingly, prodrugs with a plasma half-life close to 3 h, namely **4a** and **9a**, showed a similar kinetics curve that depicts the rapid increase of the cytoplasmic concentration of prodrug within the first two hours, followed by a quick decrease in the next five hours (Fig. 1C and 1F, respectively).

Similarly, prodrugs **9b** and **9e**, rapidly accumulated inside the cytoplasm, but their concentrations increased constantly also after 7h (Fig. 1G and 1H). This could be related to the higher stability towards plasma hydrolysis of prodrug **9b** and **9e**, with respect to **4a** and **9a**.

Assuming that the plasma cleavage of prodrugs occurred via esterase-mediated hydrolysis, the enzymatic mechanism of **4a** hydrolysis, as representative example of our prodrugs, was investigated *in vitro*. Human canboxylesterase 1 (hCE1) was chosen for two main reasons: i) its abundance in human plasma, ii) because it responsible for the hydrolysis of many clinically relevant prodrugs.[32] Since the pharmaceutical importance of hCE1 we decided to investigate the implication of the enzyme in the cleavage of prodrug **4a**. At this purpose, increasing concentrations of the compound (10, 50 and 100 μM) were incubated with a pre-warmed (37°C) mixture, containing the purified hCE1 (25 U/reaction) and 50 mM HEPES buffer pH 7.4, for 1h.

Percentage of hydrolysis was determined compared to the control (Fig. S1). As a results, it was demonstrated that **4a** is not a substrate of hCE1, being probably hydrolysed by other esterases (see Supporting Information).

Further characterization of 4a and 9a

With the purpose to select the proper pair of drug/prodrug for *in vivo* pharmacokinetics and efficacy studies, further evaluations of plasma and metabolic stability in mice, by using mouse plasma and mouse liver microsomes (MLM), were performed for prodrugs **4a** and **9a**. The rationale behind this choice is that carbamate moieties of the most common prodrugs are hydrolysed at different rates in humans and mice, because of the higher levels of esterase contained into the mouse plasma than in human plasma. Prodrugs **4a** and **9a** were incubated in mouse plasma at 37 °C, and the formation of **4*** and **9***, was monitored by UV/LC-MS, as described into the experimental section. For both the prodrugs the half-life in mouse plasma was lower than in human one ($t_{1/2}$ 1.16 h vs 3.48 h), indicating a faster hydrolysis. Moreover, **4a** and **9a** were incubated for one hour at 37 °C with a solution of mouse liver microsomes (MLM). After this time, the percentage of prodrugs and metabolites were determined. No significant differences were observed in comparison with human liver microsomes (HLM) stability (Table 4).

Table 4. Mouse Plasma stability and Mouse Liver Microsomes (MLM) stability of 4a and 9a

	Mouse Plasma $t_{1/2}$ (h)	MLM[a] Metabolic Stab.[b]%
4	-	89.2
4a	1.16	93.1
9	-	94.2
9a	2.00	93.3

[a]Mouse Liver Microsomes, [b]Expressed as percentage of unmodified drug

***In vivo* studies: pharmacokinetics and orthotopic xenograft model**

A pharmacokinetic study was performed to further investigate if the preparation of prodrugs is an effective strategy to enhance the pharmacokinetic properties of pyrazolo[3,4-*d*]pyrimidines. Drug **4** and its prodrug **4a** were chosen for this study, based on the promising cellular kinetic (Fig. 1) and physiochemical properties. The mice were divided in two groups, one receiving drug **4** (50 mg/Kg *i.p.* bolus) and the other group receiving prodrug **4a** (50 mg/Kg *i.p.* bolus). Although it is not considered a suitable solvent for *in vivo* studies, both the drug and prodrug were dissolved in DMSO, to ensure the complete solubilisation of **4**, characterized by a low solubility in other solvents. Plasma and brain tissue were collected from mice and the concentration of drug **4**, prodrug **4a** and drug **4** released by hydrolysis (from now on called **4***, in this article) was determined using HPLC analysis (Fig. 2). Prodrug **4a** showed a higher plasma concentration and a longer circulation time (Fig. 2B, **4a**) compared to drug **4** (Fig. 2A).

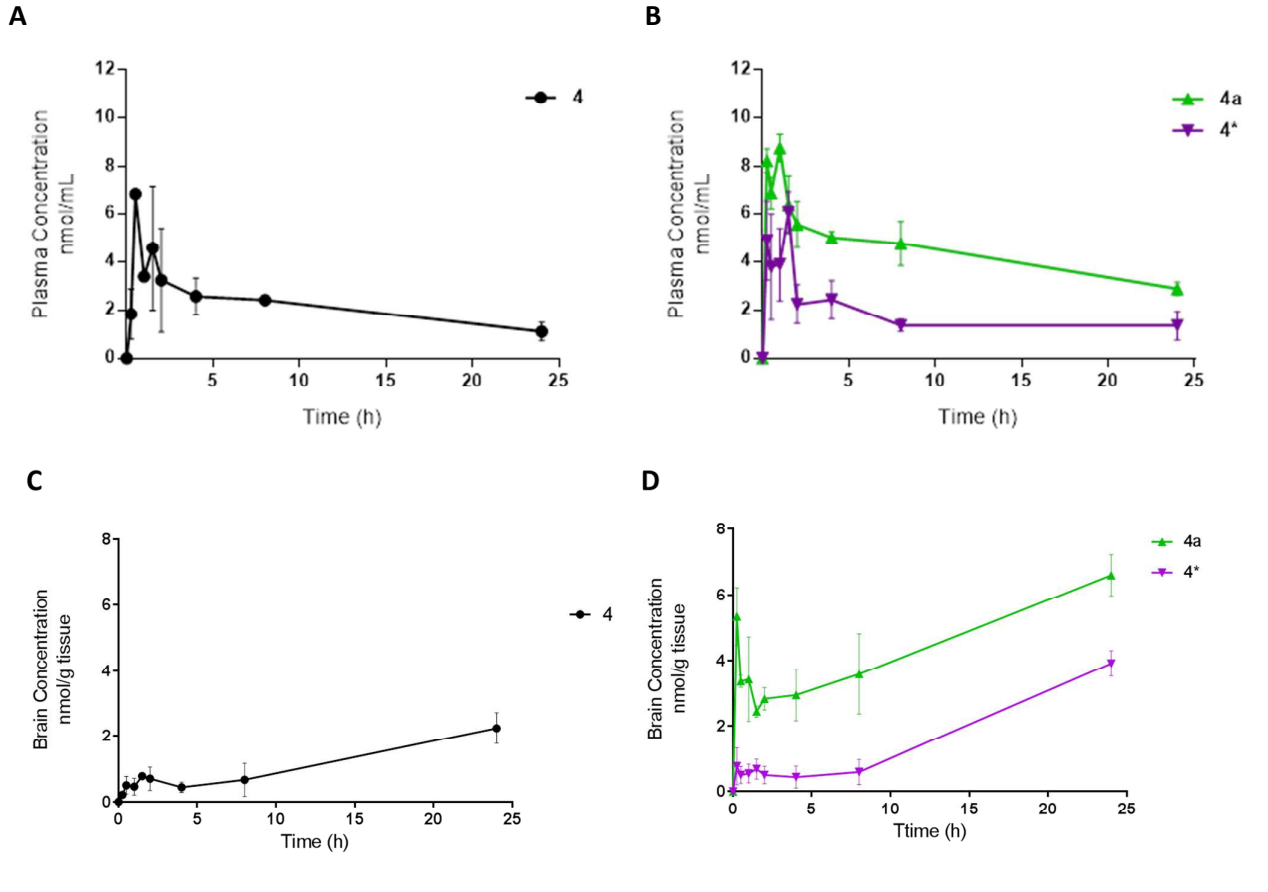

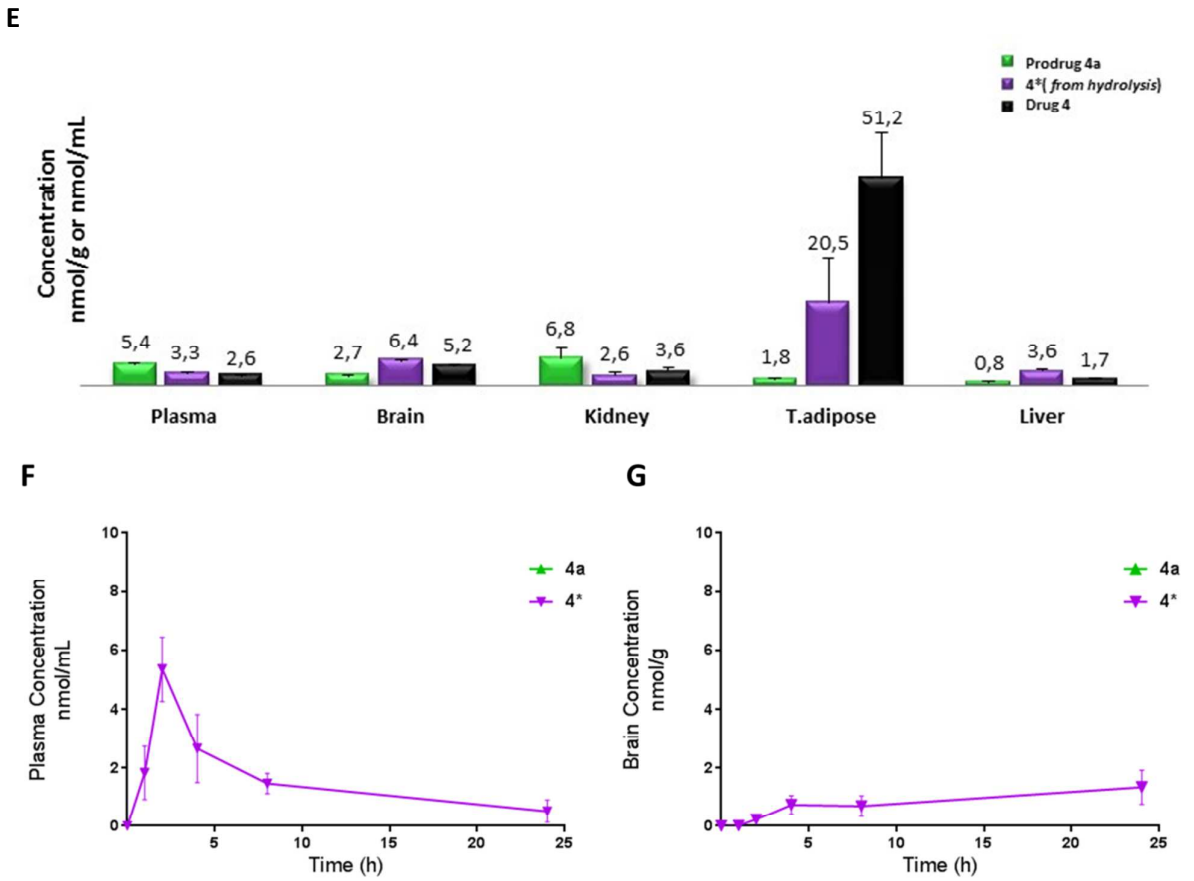

Figure 2. Pharmacokinetics of drug 4 and prodrug 4a.
A) Plasma concentration-time curve of drug **4**. B) Plasma concentration-time curve of prodrug **4a**: the green curve displays the quantity of **4a**, whereas the violet one represents the quantity of drug released from hydrolysis, **4***. C) Brain concentration-time curve of drug **4**. D) Brain concentration-time curve of prodrug **4a**: the green curve displays the quantity of **4a**, whereas the purple represents the quantity of drug released from hydrolysis, **4***. E) Biodistribution of prodrug **4a** and drug **4** at 24 h: the concentration is expressed in nmol/mL for plasma and nmol/g for the other tissues. Concentrations were determined by UV/LC-MS in plasma and brain of mice treated with compounds at a dose of 50 mg/kg (*i.p.* administration). F) Plasma concentration-time curve of **4a** after *o.s.* administration, G) Brain concentration-time curve of **4a** after *o.s.* administration.

The resulting $AUC_{0\to\infty}$ of prodrug **4a**, was 3 fold greater than the one obtained with the free drug **4** (Table 4). The concentration of drug **4** released from prodrug **4a** (Fig 2B, **4***), was comparable to the quantity of compound **4** found after administration of free drug **4** (Fig. 2A), however the $AUC_{0\to\infty}$ indicated greater plasma exposure for the drug **4***, released by the hydrolysis of prodrug **4a** (Table 4). Both compounds **4** and **4a** were able to reach the brain, with increasing concentrations during the 24 h (Fig. 2C and 2D). As for the plasma tissue, also in brain a higher

concentration of prodrug **4a**, with respect to drug **4**, was obtained (Fig. 2D, **4a**). The resulting pharmacokinetic data are shown in Table 4.

Table 4. Plasma pharmacokinetic parameters[a]

Route of Administration	**I.P. Parameters**			**O.S. Parameters**	
IP Parameters	**Drug 4**	**Prodrug 4a**	**Drug 4* *(from hydrolysis)***	**Prodrug 4a**	**Drug 4* *(from hydrolysis)***
Dose (mg/Kg)	50	50	-	50	-
Formulation	solution in DMSO	solution in DMSO	-	Methylcellulose	-
$\mathbf{C_{max}}$[b] (nmol/mL)	6.83	8.78	6.07	ND[h]	5.35
$\mathbf{T_{max}}$[c] (h)	0.50	1.00	1.50	ND[h]	2.00
MRT[d] (h)	19.15	33.34	46.62	ND[h]	11.97
AUC[e] 0→∞ (nmol∗h/mL)	79.70	264.80	135.11	ND[h]	43.53
AUC[e] 0→24h (nmol∗h/mL)	56.10	136.00	55.14	ND[h]	36.69
CL[f] (mL/min)	0.46	0.14	0.27	ND[h]	1.14
$\mathbf{t_{1/2}}$[g] (h)	14.82	23.80	33.30	ND[h]	9.06

[a]Calculated with PKCALC. [b]C_{max}: maximum concentration observed. [c]T_{max}: time of maximum concentration observed. [d]MRT: mean residence time. [e]AUC: area under the curve. [f]CL: plasma clearance. [g]$t_{1/2}$: plasma half-life. [h]Not determined, plasma levels were below the detection limits in our experimental conditions. Pharmacokinetic data were evaluated using a one-compartment model.

The antitumor properties of drug **4** and prodrug **4a** were tested in an orthotopic model of GBM. Twenty-one immunodeficient mice received intracranial injection of GBM U87 cells, and were randomly assigned to one of the three experimental groups: vehicle-treated group (control); drug-treated group (receiving 50 mg/Kg of **4**); prodrug-treated group (receiving 50 mg/Kg of **4a**).

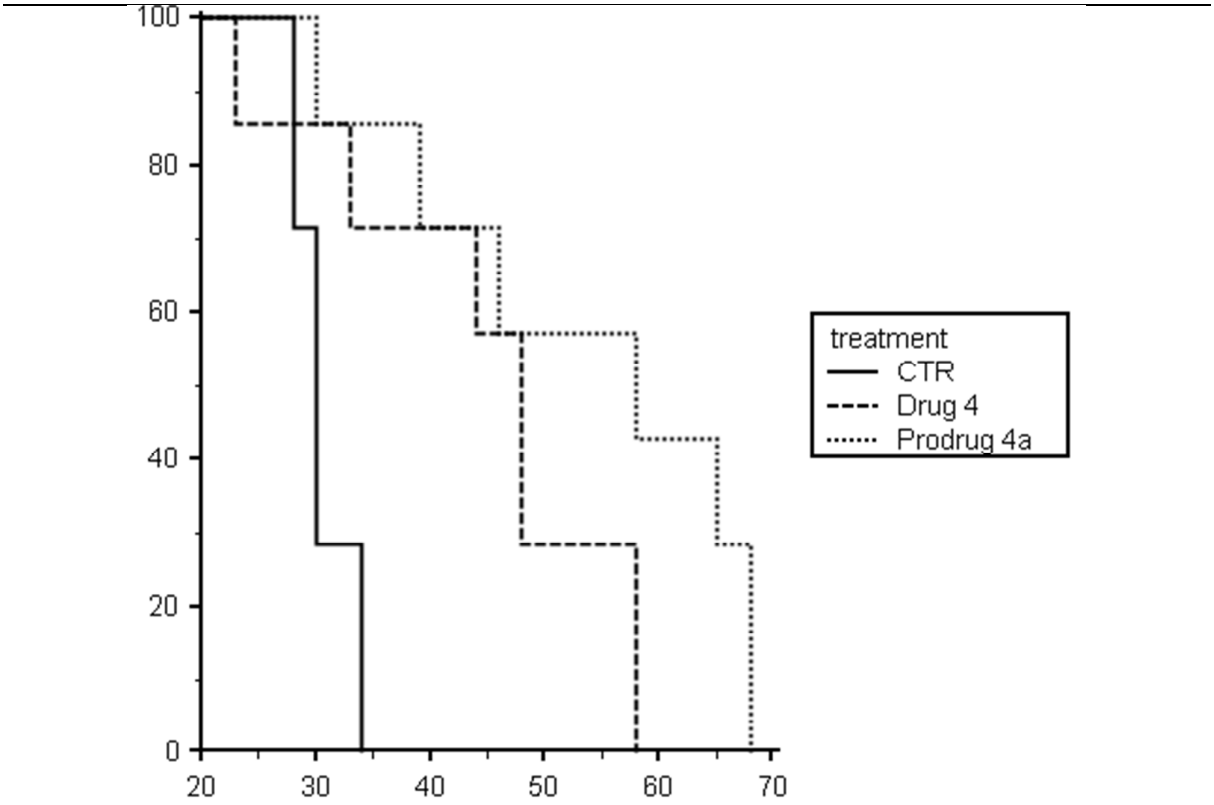

Figure 3. Orthotopic mouse model of GBM: survival curves for mice treated with vehicle (CTR), drug 4 and prodrug 4a.

Each group initially contained 7 mice. Mice received every other day oral administration of methylcellulose vehicle (CTR), 50 mg/kg of compound **4** or 50 mg/kg of prodrug **4a**. Compound **4** and its prodrug **4a** were prepared as suspension in 0.5% methylcellulose solution.

All mice died within 68 days after cell injection, but survival curves demonstrated that mice receiving drug **4** or prodrug **4a** had a longer life expectancy compared with vehicle-treated mice (Fig. 3). In fact, median survival time was 44 days for the mice treated with drug **4**, 49 days for the group that received prodrug **4a** and 30 days for the control group (Table 5). In addition, the survival time data showed a statistically significant difference between the group treated with drug **4** and the group that received prodrug **4a**, with a small but substantial increase in the survival time in the second group.

In order to strengthen results from *in vivo* tumor model and study the PK/PD correlation for prodrug **4a**, pharmacokinetics parameters were also evaluated after oral administration (*o.s.*). Mice received a single dose of 50 mg/Kg **4a** as suspension in 0.5 % methylcellulose solution.

Plasma and brain tissues were collected at 5 time points during 24 h and the amount of **4a** and **4*** was determined by HPLC analysis. The calculated pharmacokinetics parameters are shown in Table 4. Prodrug **4a** was not detected neither in the plasma nor in the brain, probably because of its complete hydrolysis into the GI. On the other hand, it was observed an increasing concentration of **4*** both in the plasma and brain (Fig. 2F and Fig. 2G) with a C_{max} in the plasma tissue reached after 2 h (T_{max}). The $AUC_{0\rightarrow\infty}$ of **4*** from hydrolysis was lower than the one observed for **4** administrated by *i.p.*, about the half, while the C_{max} resulted comparable.

Table 5. *In vivo* antitumor efficiency: median survival time and statistics

Group	Median survival (days)	95% CI for the median	P (*vs* CTR)	P (*vs* drug 4)
CTR	30	28-34	-	-
Drug 4	44	33-48	0.0114*	-
Prodrug 4a	49	42-59	<0.01*	0.0397

*P<0.05 was considered statistically significant, P according to Logrank test.

DISCUSSION

Compounds **1-9** were selected for this study, among the pyrazolo[3,4-*d*]pyrimidines of our in-house library as they offer a suitable balance between the already reported *in vitro* activity and ADME properties, together with several different chemical features at the N1, C4 and C6 positions.[5,13,26-29] Particularly position C4, which contains the group involved in the formation of the carbamate group, required to link the prodrug moiety to the pyrazolo[3,4-*d*]pyrimidines. To develop an efficient synthesis and demonstrate its versatility, it was therefore important to select derivatives with suitable chemical diversity at C4. The NH-group at the C4 position was chosen as the group to link the prodrug-moiety as it is the easiest group to access chemically and the most shared feature within the pyrazolo[3,4-*d*]pyrimidine library (i.e. it creates crucial bonds within the ATP binding site of the tyrosine kinase).[33] To improve the low aqueous solubility of compounds **1-9**, *N*-methylpiperazine was selected as the 'solubilizing' prodrug group for its characteristic of being protonated at physiological conditions.[34] *N*-methylpiperazine was attached by an *in vivo* hydrolysable ethylcarbamate-linker to the C4 position of the pyrazolo[3,4-*d*]pyrimidine nucleus.[34]

In this study, we first improved the prodrug synthesis previously reported which involved two separate steps and the isolation of the unstable carbamic-chloride intermediate, resulting in medium to low yields of final prodrugs.[22] The new synthesis was instead performed in a one-pot, two-step fashion starting from the appropriate pyrazolo[3,4-*d*]pyrimidine (**1-9**) with the addition of trisphogene and sodium bicarbonate. Once the carbamic-chloride intermediate was formed (1-5h), the appropriate alcohol (**12,13** and **17-19**) was added (Scheme 1). This synthesis provided better yields (i.e. for **9a**) and has proven to be an effective strategy to introduce the prodrug moiety in several pyrazolo[3,4-*d*]pyrimidines bearing different chemical features. For instance, the secondary amino group at C4, which is directly involved in the carbamate group formation, showed alkyl, substituted-phenyl, phenylethyl and benzylic groups. This synthetic approach

further demonstrated its versatility in the synthesis of the final prodrugs **9b-9e**, where alcohols more sterically hindered than **12**, were used (**13** and **17-19**) (Scheme 2). These alcohols (**13** and **17-19**) were used to generate a series of prodrugs with increasing steric hindrance in proximity of the carbamate linker. Alcohols **12,13** and **17-19**, bearing H, Me, Et, Ph and Bn as substituent in position 1, were prepared using different procedures, as described in Scheme 3.

Aqueous solubility, stability in methanol, phosphate buffer and plasma were investigated, as well as metabolic stability (HLM) and permeability (PAMPA). Prodrugs' data regarding solubility, stability and permeability are shown in Table 2 and Table 3, together with the data obtained from their parent drugs, for comparison. The stability of the prodrugs was initially determined by UV/LC−MS in methanol and phosphate buffer (PBS, pH 7.4) to evaluate if the contribution of chemical hydrolysis induced by these polar media was minimal with respect to the rate of hydrolysis measured in subsequent plasma stability test. Prodrugs (**1a-7a**, **9a-c**, **9e**) demonstrated a good stability profile in the polar solutions tested and were consequently regarded as chemically stable for the subsequent evaluation of their susceptibility to enzymatic hydrolysis. On the contrary, the stability of prodrugs **8a** and **9d** was too low to further test these compounds regarding their aqueous solubility, metabolic stability and permeability.

Prodrugs are usually defined as bioreversible derivatives of active drugs and, in this regard, our strategy was to synthesize prodrugs with a carbamate moiety, potentially cleavable by *in vivo* hydrolases.[35] To confirm the hypothesis, all synthesized prodrugs were tested for their stability in human plasma and the rate of hydrolysis was monitored by UV/LC-MS. Results demonstrated that all tested prodrugs were converted into the corresponding active drugs. As the half-lives ranged from 0.46 to 75.0 h, a potential connection between the rate of hydrolysis and the substituent at the C4 position of the pyrazolo[3,4-*d*]pyrimidines was investigated. The analysis showed that compounds with a benzyl or phenylethyl amine at C4 (**1a**, **2a**, **5a** and **9e**) demonstrated a very high

stability, whereas compounds having a C4-aniline group, lead to prodrugs more susceptible to plasma hydrolysis (**3a**, **4a**, **6a**, **7a** and **9a**). Prodrug **8a**, with an *n*-butylamino moiety at C4, was already reported for its low half-life in plasma. Prodrugs **9b-9e**, which show an increasing steric bulk in proximity of the hydrolysable centre, were investigated to further understand if steric hindrance could determine a remarkable difference in the rate of enzymatic hydrolysis. Results demonstrated that the bulkier the substituent R^5 of the linker, the greater the plasma half-life of the prodrug (H<Me<Et<Bn = **9a**<**9b**<**9c**<**9e** = 3.21 h<10.4 h<11.3 h<40.0 h). A possible explanation is that the steric hindrance generated by the substituent close to the centre of hydrolysis, namely the carbamate group, could hurdle the access of plasma hydrolytic enzymes. To understand if metabolism of prodrugs could involve CYP-oxidative pathways, the compounds were incubated with HLM for 1 h and their concentration within the samples was monitored by UV/LC-MS. The percentage of unmodified prodrug was in general very high (86.4% was the lowest value obtained (**1a**)) and the metabolite patterns generated from prodrugs were similar to those obtained from the respective drugs. These data support the hypothesis that prodrugs and prodrug-linkers do not represent a direct substrate of CYP-metabolism. The analysis of thermodynamic solubility demonstrated the enhanced aqueous solubility of each prodrug in comparison to the respective drug, validating the synthesis of prodrugs as a strategy to overcome the poor aqueous solubility of pyrazolo[3,4-*d*]pyrimidines.

Prodrugs are chemically modified version of an active drug and typically, bioconversion (from prodrug to drug) is required for the interaction with the drug's biological target. [24,25] Pyrazolo[3,4-*d*]pyrimidines have been studied for their inhibitory activity towards tyrosine kinases activated in cancer such as c-Abl and c-Src. This activity is related to the interactions that most of these compounds create within the tyrosine kinases ATP-binding site. In order to understand if the herein synthesized prodrugs were able to interact directly with c-Abl and c-Src, a cell-free assay

was set up. As confirmation of the data previously reported regarding **9a**, also prodrugs **4a**, **9b** and **9e** were not able to inhibit these tyrosine kinases at the maximum concentration tested (100 μM). These results seemed to support the hypothesis that prodrugs cannot directly establish interactions within the ATP-binding site (i.e. the prodrug-linker masks the C4 secondary amino group that is required to create favorable bonds).[33]

Theoretically, prodrugs acquire antitumor activity after the hydrolysis-mediated release of the parent drug (hydrolysis of the *O*-alkyl-carbamate linker was demonstrated by plasma hydrolysis studies). Accordingly, a cellular assay with human GBM U87 cells was performed to assess the cytotoxicity of our prodrugs and to compare their activity with the one of their respective drugs. Nearly all the prodrugs tested (**4a**, **6a**, **7a**, **9a-c**, **9e**) were more active than the respective drug at 24 h, a result potentially related to the involvement of different cellular uptake mechanisms for drug and prodrug. The only exception was prodrug **1a** whose high resistance to hydrolysis might justify the different behavior at 24h. The difference in cytotoxicity within each pair of drug and prodrug decreased at 48 h and, consistently with this trend, drug and respective prodrug showed the same values of IC_{50} at 72 h.

The cellular kinetics of the series of 'chemically' modified prodrugs **9a-c**, **9e** and of **4a** were also studied (Fig. 1). The series **9a-c**, **9e** was included to understand the behavior towards hydrolysis and cellular uptake of compounds with increasing hindrance close to the hydrolysable group, whereas prodrug **4a** was selected for this test because of the plasma half-life value obtained, lower than 24 h, and the activity towards U87 cells. Further, since drugs **4** and **9** were the most and the least water soluble, it was interesting to analyze their behavior in cells in comparison to their more soluble prodrugs, namely **4a** and **9a**. Prodrugs showed an improved ability of entering into U87 cells, as demonstrated by the faster uptake and the quantity of prodrug measured into the cytoplasm. These data, together with the cytotoxicity values at 24 h, suggest that prodrug

treatment is associated with an increased availability of the active drug into the cellular compartment where the inhibition of biological target takes place. Nevertheless, the measured concentration of drug released by hydrolysis was comparable to the one obtained by treatment with the active drug; these data might be explained by a higher retention of the drug in cell membrane respect to the prodrug. Noticeably the IC_{50} at 72 h, showed the comparable activity of drugs and respective prodrugs, demonstrating that both drug and prodrug during the 72 h are able to reach the concentration needed to determine an equal cytotoxicity.

In order to gain a deeper insight into the mechanism of hydrolysis of our prodrugs, the representative **4a** was selected for being studied as possible substrate of human carboxylesterase 1 (hCE1). hCE1 was chosen because of its clinical relevance, indeed it is responsible of the hydrolysis and activation of different prodrugs.[32] From our results, hCE1 did not demonstrate to be implicated into the mechanism of **4a** hydrolysis (see Supporting Informations), probably being another esterase responsible for the cleavage of our pyrazolo[3,4-*d*]pyrimidines prodrugs.

To evaluate if the preparation of prodrugs can enhance the pharmacokinetic properties of a poorly water-soluble drug, a proof of concept *in vivo* study was performed (Fig. 2). Drug **4** and prodrug **4a** were selected for this purpose taking into account all the properties previously assessed. Moreover, the stability in mouse plasma was studied to have an idea of the hydrolysis rate of **4a** in mice. As expected, **4a** was faster hydrolyzed (Table 4) in mouse plasma than in human plasma and its metabolic stability after incubation with mouse liver microsomes (MLM) did not show substantial differences.

In vivo exploratory pharmacokinetics studies where than performed on the selected pair **4**/**4a**. Remarkably, in the group of mice treated with prodrug **4a**, the quantity of prodrug measured in plasma was 2 fold higher than the quantity of drug inside the plasma of mice treated with the free drug **4** (Fig. 2A and 2B). The measured plasma concentration and the resulting $AUC_{0\rightarrow 24h}$ of drug

4*, released by hydrolysis of prodrug **4a**, were comparable to those obtained by administration of the free drug **4**. However, it is worth to notice that the $AUC_{0\rightarrow\infty}$ of the drug released form hydrolysis **4*** (value of 135.11 nmol h/mL) was twice as high as the value obtained with the administration of free drug **4** (79.7 nmol h/mL). These data suggests that prodrug **4a**, allows for a slow release of drug **4***, guaranteeing a prolonged overall exposure to the active compound. The pharmacokinetics in the brain compartment were also investigated, as the assessment of the cellular activity of these compounds was performed in human GBM U87 cell line (Fig. 2C and 2D). The concentration of prodrug **4a** quantified into the brain was higher than the quantity of drug **4** measured in the brain of mice treated only with the free drug (**4**). Moreover, the curve obtained indicates that after 24 h the prodrug still accumulates within the brain, suggesting that the tumor site will have a prolonged exposure to prodrug **4a** and, consequently to hydrolysis, also to active drug **4***.

The efficacy of **4** and **4a** was further studied in an orthotopic mouse model of GBM. The groups of mice treated with both drug **4** and prodrug **4a** showed a benefit in cancer survival with respect to the vehicle-treated mice. In addition, treatment with prodrug **4a** resulted in a minor but significant increase in median survival time. These results are in agreement with our previous data regarding the antitumor activity of drug **4** in GBM.

Driven by the efficacy data obtained from orthotopic models, the PK profile of **4a** administrated by *o.s.* was finally evaluated. Mice were treated with a single dose of **4a** 50 mg/Kg in 0.5% of methylcellulose. Differently from *i.p.* injection, the prodrug was not detected neither in the plasma tissue nor in the brain probably because of a complete hydrolysis occurred in the GI. Indeed, only **4*** (from hydrolysis) was found into the plasma showing a PK profile comparable to the one of **4** after *i.p.* administration. Overall, the observed blood exposure of **4*** appeared to be slightly lower after o.s. administration. Noteworthy, it was observed a slow accumulation of **4*** into the brain

which most likely resulted in an increased exposure of the brain after repeated administrations in the efficacy studies.

The improved biological activity, demonstrated *in vivo* after administration of prodrug **4a** with respect to drug **4**, suggest that prodrug **4a** could represent an effective step forward in the development of drug **4**.

CONCLUSIONS

In the present study we advanced our synthetic strategy to produce prodrugs of a variety of pyrazolo[3,4-*d*]pyrimidines in an easy and versatile fashion. The synthesized prodrugs displayed improved aqueous solubility and good metabolic stability. The hydrolysis of the prodrugs was confirmed in plasma, where the active drugs were released by enzymatic cleavage of the carbamate prodrug-moiety. Cellular kinetics further supported the hydrolysis of prodrugs and showed a quicker uptake process for prodrugs in comparison to their respective drugs. The cytotoxicity at 72 h of the drugs and prodrugs tested were comparable, suggesting the complete release of the active drug. At the end, as *in vivo* proof of concept, the pharmacokinetics and efficacy of the most promising pair of drug/prodrug were studied. In comparison to the parent drug **4**, prodrug **4a** demonstrated a comparable efficacy in a pivotal *in vivo* study, with a slightly increasing, but worthy of further investigations, of the median survival time of mice in an orthotopic GBM model. All together these results demonstrate the success of the application of the studied prodrug approach to pyrazolo[3,4-*d*]pyrimidine compounds with the aim of improving their poor water solubility, determining a positive impact also in their biological efficacy.

EXPERIMENTAL SECTION

Synthesis and characterization of compounds

Compounds **1-9** were previously synthesized and published by our group.[5,13,26-29]

All commercially available chemicals were used as purchased from Sigma Aldrich. DCM was dried over sodium hydride. Anhydrous reactions were run under a positive pressure of dry N_2. TLC was carried out using Merck TLC silica gel 60 F_{254}. Chromatographic purifications were performed on columns packed with Merck silica gel 60, 23-400 mesh, for flash technique. ^{1}H NMR and ^{13}C NMR spectra were recorded at 400 MHz on a Bruker Avance DPX400. Chemical shifts are reported relative to tetramethylsilane at 0.00 ppm. Mass spectra (MS) data were obtained using an Agilent 1100 LC/MSD VL system (G1946C) with a 0.4 mL/min flow rate using a binary solvent system of 95/5 = MeOH/H_2O. UV detection was monitored at 254 nm. MS were acquired in positive and negative mode scanning over the mass range 100-1500. The following ion source parameters were used: drying gas flow, 9 mL/min; nebulizer pressure, 40 psi; drying gas temperature, 350 °C.

All target compounds possessed a purity of ≥ 95% verified by UV/LC-MS method as reported in the "UV/HPLC-MS method" section below.

General procedure for the synthesis of pyrazolo[3,4-d]pyrimidine prodrugs (1a-8a, 9a-e)

$NaHCO_3$ (2.25 mmol, 5.00 eq.) was added to a solution of the appropriate pyrazolo[3,4-*d*]pyrimidine compound (**1-9**) (0.45 mmol, 1.00 eq.) in DCM_{dry} (8 mL). After 5 min of stirring at r.t., the suspension was cooled with an ice-bath, then a solution of triphosgene (0.45 mmol, 1.00 eq.) in DCM_{dry} (8 mL) was added. After 30 min the ice-bath was removed and the reaction mixture was allowed to warm to r.t. and stirred until the spot of the starting material disappeared on TLC (2 h, approximately). A solution of alcohol (**10-14**) (0.90 mmol, 2.00 eq.) in DCM_{dry} (8 mL) was added and the resulting mixture was stirred at r.t. for 16 h. The solvent was evaporated under reduced

pressure and the resulting residue was purified by flash chromatography using a mixture of DCM and MeOH as eluent.

2-(4-methylpiperazin-1-yl)ethyl benzyl1-(2-chloro-2-phenylethyl)-1H-pyrazolo[3,4-*d*]pyrimidin-4-ylcarbamate (1a)

Colourless oil. Yield: 79%. ^{1}H-NMR ($CDCl_3$) δ (ppm): 8.65 (s, 1H), 8.26 (s, 1H), 7.39 (d, *J* = 7.6 Hz, 2H), 7.24 (m, 8H), 5.52 (dd, *J* = 6, 8.4 Hz, 1H), 5.35 (s, 2H), 5.02 (dd, *J* = 8.8, 14.4 Hz, 1H), 4.79 (dd, *J* = 6, 14 Hz, 1H), 4.33 (t, *J* = 5.6 Hz, 2H), 2.55 (t, *J* = 5.6 Hz, 2H), 2.40 (m, 8H), 2.24 (s, 3H). ^{13}C-NMR ($CDCl_3$) δ (ppm): 154.7, 154.1, 154.0, 137.7, 135.7, 128.7, 128.5, 128.2, 128.1, 127.1, 127.0, 106.3, 63.9, 60.1, 56.3, 54.8, 53.7, 52.9, 49.9, 45.8. MS (ES) *m/z*: 535 $[M+H]^+$.

2-(4-methylpiperazin-1-yl)ethyl 2-chlorobenzyl1-(2-(4-bromophenyl)-2-chloroethyl)-1H-pyrazolo[3,4-*d*]pyrimidin-4-ylcarbamate (2a)

Colourless oil. Yield: 76% ^{1}H-NMR ($CDCl_3$) δ (ppm): 8.62 (s, 1H), 8.31 (s, 1H), 7.42 (d, *J* = 8.4 Hz, 2H), 7.18 (m, 6H), 5.50 (m, 1H), 5.44 (s, 2H), 4.99 (m, 1H), 4.82 (m, 1H), 4.34 (t, *J* = 5.2 Hz, 2H), 2.54 (t, *J* = 5.6 Hz, 2H), 2.41 (m, 8H), 2.26 (s, 3H). ^{13}C-NMR ($CDCl_3$) δ (ppm): 154.7, 154.6, 154.2, 136.7, 135.8, 135.1, 132.3, 131.7, 129.2, 128.9, 128.0, 127.0, 126.6, 122.8, 106.1, 64.3, 59.0, 56.2, 54.7, 53.4, 52.7, 48.1, 45.6, 29.5. MS (ES) *m/z*: 648 $[M+H]^+$, 670 $[M+Na]^+$.

2-(4-methylpiperazin-1-yl)ethyl 3-chlorophenyl6-(methylthio)-1-phenethyl-1H-pyrazolo[3,4-*d*]pyrimidin-4-ylcarbamate (3a)

Colourless oil. Yield: 75%. ^{1}H-NMR ($CDCl_3$) δ (ppm): 7.93 (s, 1H), 7.35 (d, *J* = 4.8 Hz, 2H), 7.22 (m, 7H), 4.62 (t, *J* = 7.6 Hz, 2H), 4.39 (t, *J* = 5.2 Hz, 2H), 3.22 (t, *J* = 7.6 Hz, 2H), 2.60 (t, *J* = 5.2 Hz, 2H), 2.47 (m, 8H), 2.32 (S, 3H), 2.28 (s, 3H). ^{13}C-NMR ($CDCl_3$) δ (ppm): 168.2, 155.2, 153.7, 153.1, 140.8, 137.8, 134.3, 134.1, 129.6, 129.4, 129.1, 128.7, 128.4, 127.9, 127.0, 126.7, 126.6, 103.2, 64.5, 63.8, 56.2, 54.8, 52.7, 48.3, 48.1, 45.6, 45.5, 35.1. MS (ES) *m/z*: 567 $[M+H]^+$.

2-(4-methylpiperazin-1-yl)ethyl 6-(2-morpholinoethylthio)-1-(2-chloro-2-phenylethyl)-1H-pyrazolo[3,4-*d*]pyrimidin-4-yl3-bromophenylcarbamate (4a)

Colourless oil. Yield: 51%. ^{1}H-NMR ($CDCl_3$) δ (ppm): 7.95 (s, 1H), 7.48 (d, *J* = 8 Hz, 1H), 7.42 (m, 3H), 7.29 (m, 4H), 7.15 (d, *J* = 8.4 Hz, 1H), 5.51 (t, *J* = 6 Hz, 1H), 4.94 (dd, *J* = 8.8, 14 Hz, 1H), 4.71 (dd, *J* = 6, 14 Hz, 1H), 4.35 (t, *J* = 5.2 Hz, 2H), 3.69 (t, *J* = 4.4 Hz, 4H), 3.01 (m, 2H), 2.49 (m, 19H), 2.27 (s, 3H). ^{13}C-NMR ($CDCl_3$) δ (ppm): 168.1, 155.8, 153.9, 153.0, 140.8, 137.7, 135.2, 131.8, 130.9, 130.0, 128.8, 128.5, 127.4, 127.1, 121.9, 103.2, 77.1, 76.8, 76.5, 66.7, 64.5, 59.9, 57.4, 56.2, 54.8, 53.3, 53.2, 52.8, 45.6, 31.7, 30.7, 29.5, 29.1, 27.9. MS (ES) *m/z*: 745 $[M+H]^+$, 767 $[M+Na]^+$.

2-(4-methylpiperazin-1-yl)ethyl 1-(2-chloro-2-phenylethyl)-6-(methylthio)-1H-pyrazolo[3,4-*d*]pyrimidin-4-ylphenethylcarbamate (5a)

Colourless oil. Yield: 71%. ^{1}H-NMR ($CDCl_3$) δ (ppm): 8.06 (s, 1H), 7.41 (d, *J* = 6.4 Hz, 2H), 7.24 (m, 8H), 5.51 (t, *J* = 8 Hz, 1H), 4.93 (dd, *J* = 8, 14 Hz, 1H), 4.78 (dd, *J* = 6.8, 14.4 Hz, 1H), 4.30 (m, 4H), 3.02 (t, *J* = 7.6 Hz, 2H), 2.65 (m, 11H), 2.38 (s, 3H). ^{13}C-NMR ($CDCl_3$) δ (ppm): 168.7, 155.7, 154.1, 138.7, 138.0, 136.1, 129.0, 128.7, 128.5, 127.4, 126.5, 103.7, 63.6, 60.1, 56.4, 54.7, 53.8, 52.3, 48.8, 45.4, 35.1, 29.7, 14.3. MS (ES) *m/z*: 595 $[M+H]^+$.

2-(4-methylpiperazin-1-yl)ethyl 1-(2-(4-bromophenyl)-2-chloroethyl)-1H-pyrazolo[3,4-*d*]pyrimidin-4-ylphenylcarbamate (6a)

Colourless oil. Yield: 25%. ^{1}H-NMR ($CDCl_3$) δ (ppm): 8.61 (s, 1H), 7.77 (s, 1H), 7.42 (m, 4H), 3.76 (m, 5H), 5.48 (t, *J* = 8 Hz, 1H), 4.97 (dd, *J* = 8.4, 14 Hz, 1H), 4.80 (dd, *J* = 6.4, 14 Hz, 1H), 4.36 (t, *J* = 5.6 Hz, 2H), 2.57 (t, *J* = 5.6 Hz, 2H), 2.43 (m, 8H), 2.31 (S, 3H). ^{13}C-NMR ($CDCl_3$) δ (ppm): 155.6, 155.0, 154.7, 153.6, 139.9, 136.8, 135.0, 131.9, 129.1, 128.7, 128.3, 123.1, 106.1, 65.2, 64.8, 59.2, 56.3, 56.2, 54.8, 54.7, 53.6, 53.4, 52.4, 45.5, 30.3, 29.7. MS (ES) *m/z*: 598 $[M+H]^+$, 620 $[M+Na]^+$.

2-(4-methylpiperazin-1-yl)ethyl (1-(2-chloro-2-phenylethyl)-6-(methylthio)-1*H*-pyrazolo[3,4-*d*]pyrimidin-4-yl) 3-chlorophenylcarbamate (7a)

Colourless oil. Yield: 85%. ^{1}H-NMR ($CDCl_3$) δ (ppm): 7.95 (s, 1H), 7.40 (d, *J* = 6.8 Hz, 2H), 7.29 (m, 6H), 7.11 (m, 1H), 5.50 (t, *J* = 7.0 Hz, 1H), 4.93 (dd, *J* = 8.4, 14 Hz, 1H), 4.76 (dd, *J* = 6.4, 14 Hz, 1H), 4.35 (t, *J* = 5.2 Hz, 2H), 2.55 (t, *J* = 5.2 Hz, 2H), 2.41 (m, 8H), 2.27 (s, 3H), 2.26 (s, 3H). ^{13}C-NMR ($CDCl_3$) δ (ppm): 168.6, 155.8, 153.7, 153.1, 140.6, 137.7, 135.2, 134.1, 129.6, 129.0, 128.8, 128.5, 127.9, 127.2, 126.9, 103.0, 64.6, 59.8, 56.2, 54.8, 53.6, 52.8, 45.7, 29.5. MS (ES) *m/z*: 601 $[M+H]^+$.**2-(4-methylpiperazin-1-yl)ethyl butyl1-(2-chloro-2-phenylethyl)-6-(ethylthio)-1H-pyrazolo[3,4-*d*]pyrimidin-4-ylcarbamate (8a)**

Colourless oil. Yield: 39%. ^{1}H-NMR ($CDCl_3$) δ (ppm): 8.08 (s, 1H), 7.39 (d, *J* = 6.8 Hz, 2H), 7.27 (m, 3H), 5.50 (t, *J = 7.6* Hz, 1H), 4.91 (dd, *J* = 8.4, 14.4 Hz, 1H), 4.76 (dd, *J* = 6.4, 14 Hz, 1H), 4.37 (t, *J* = 5.6 Hz, 2H), 4.03 (t, *J* = 7.6 Hz, 2H), 3.17 (q, *J* = 7.2 Hz, 2H), 2.67 (t, *J* = 5.6 Hz, 2H), 2.54 (m, 8H), 2.31 (s, 3H), 1.66 (q, *J* = 7.6 Hz, 2H), 1.43 (t, *J* = 7.2 Hz, 3H), 1.31 (m, 3H), 0.93 (t, *J* = 7.1 Hz, 3H). ^{13}C-NMR ($CDCl_3$) δ (ppm): 168.2, 155.7, 154.4, 154.4, 138.1, 136.1, 128.9, 128.7, 127.4, 104.0, 63.9, 60.1, 56.6, 55.1, 53.8, 53.2, 47.3, 46.0, 30.9, 29.7, 25.4, 20.1, 14.7, 13.9. MS (ES) *m/z*: 561 $[M+H]^+$.

2-(4-methylpiperazin-1-yl)ethyl 3-bromophenyl6-(methylthio)-1-(2-phenylpropyl)-1H-pyrazolo[3,4-*d*]pyrimidin-4-ylcarbamate (9a)

Colourless oil. Yield: 30%.^{1}H-NMR ($CDCl_3$) δ (ppm): 7.88 (s, 1H), 7.49 (d, *J* = 8 Hz, 1H), 7.42 (s, 1H), 7.12 (m, 7H), 4.49 (t, *J* = 7.5 Hz, 2H), 4.35 (t, *J* = 5.2 Hz, 2H), 3.53 (m, 1H), 2.55 (m, 10H), 2.35 (s, 3H), 2.8 (s, 3H)1.41 (s, 3H). ^{13}C-NMR ($CDCl_3$) δ (ppm): 175.5, 168.4, 155.8, 153.9, 153.3, 141.0, 134.5, 132.0, 131.1, 130.2, 128.5, 127.6, 127.2, 126.8, 122.1, 103.2, 64.6, 56.1, 54.0, 53.8, 51.8, 44.5, 39.9, 21.8, 18.8, 14.1. MS (ES) *m/z*: 626 $[M+H]^+$, 648 $[M+Na]^+$.

1-(4-methylpiperazin-1-yl)propan-2-yl 3-bromophenyl6-(methylthio)-1-(2-phenylpropyl)-1H-pyrazolo[3,4-*d*]pyrimidin-4-ylcarbamate (9b)

Colourless oil. Yield: 30%.^{1}H-NMR ($CDCl_3$) δ (ppm): 7.88 (s, 1H), 7.46 (m, 2H), 7.24 (m, 5H), 7.16 (m, 2H); 5.20 (m, 1H), 4.50 (m, 2H), 3.52 (q, J = 7.2 Hz, 1H), 2.45 (m, 10H), 2.33 (s, 3H), 2.28 (s, 3H),

1.22 (m, 6H). ^{13}C-NMR ($CDCl_3$) δ (ppm): 168.1, 155.5, 153.9, 152.9, 143.1, 141.1, 134.29, 131.8, 130.6, 129.8, 128.2, 127.3, 127.0, 126.5, 121.7, 103.15, 71.0, 62.6, 54.8, 53.5, 52.7, 45.4, 39.7, 29.5, 18.5, 17.9. MS (ES) *m/z*: 639 $[M+H]^+$.

1-(4-methylpiperazin-1-yl)butan-2-yl 3-bromophenyl6-(methylthio)-1-(2-phenylpropyl)-1H-pyrazolo[3,4-*d*]pyrimidin-4-ylcarbamate (9c)

Colourless oil. Yield: 40%.^{1}H-NMR ($CDCl_3$) δ (ppm): 7.90 (s, 1H), 7.46 (m, 2H), 7.24 (m, 5H), 7.16 (m, 2H); 5.08 (m, 1H), 4.50 (m, 2H), 3.52 (q, *J* = 6.8 Hz, 1H), 2.50 (m, 12H), 2.29 (s, 3H), 2.27 (s, 3H), 1.23 (s, 3H), 0.88 (m, 3H). ^{13}C-NMR ($CDCl_3$) δ (ppm): 170.2, 155.4, 154.0, 153.2, 143.1, 141.1, 134.4, 131.8, 130.5, 129.7, 128.2, 127.3, 127.0, 126.5, 121.7, 103.4, 75.4, 61.0, 54.9, 53.5, 45.6, 39.7, 29.5, 25.1, 18.5, 13.9, 9.34. MS (ES) *m/z*: 652 $[M+H]^+$.

2-(4-methylpiperazin-1-yl)-1-phenylethyl 3-bromophenyl6-(methylthio)-1-(2-phenylpropyl)-1H-pyrazolo[3,4-*d*]pyrimidin-4-ylcarbamate (9d)

Colourless oil. Yield: 32%.^{1}H-NMR ($CDCl_3$) δ (ppm): 7.74 (s, 1H), 7.54 (d, J = 8 Hz, 1H), 7.46 (s, 1H), 7.21 (m, 12H), 6.00 (d, *J* = 8.8 Hz, 1H); 4.48 (m, 2H), 3.53 (q, *J* = 6.8 Hz, 1H), 2.88 (bs, 6H), 2.72 (m, 7H), 2.31 (s, 3H), 1.25 (s, 3H). ^{13}C-NMR ($CDCl_3$) δ (ppm): 168.4, 155.7, 153.9, 152.8, 143.3, 141.2, 137.6, 134.4, 132.1, 131.1, 130.3, 128.7, 127.4, 127.2, 126.8, 126.3, 122.0, 103.2, 75.4, 63.2, 54.4, 53.8, 51.2, 44.4, 39.9, 29.7, 25.1, 18.7. MS (ES) *m/z*: 652 $[M+H]^+$.

1-(4-methylpiperazin-1-yl)-3-phenylpropan-2-yl 3-bromophenyl-6-(methylthio)-1-(2-phenylpropyl)-1H-pyrazolo[3,4-*d*]pyrimidin-4-ylcarbamate (9e)

Colourless oil. Yield 52% ^{1}H NMR ($CDCl_3$) δ (ppm)= 7.75 (s, 1H), 7.55-7.53 (d, 1H), 7.46 (s, 1H), 7.31-7.13 (m, 12H), 6.01-5.99 (m, 1H), 4.54-4.43 (m, 2H), 3.55-3.50 (m, 1H), 2.88 (m, 6H), 2.78 (m, 2H), 2.72-2.56 (m, 7H), 2.31 (m, 3H), 1.25 (m, 3H). ^{13}C-NMR ($CDCl_3$) δ (ppm): 168.4, 155.7, 153.9, 152.8, 142.4, 141.2, 137.6, 134.4, 132.1, 131.1, 130.3, 128.7, 127.4, 127.2, 126.8, 126.3, 122.0, 103.2, 78.3, 63.2, 54.4, 53.8, 51.2, 44.4, 39.9, 38.4, 29.7, 25.1, 18.7. MS (ES): *m/z*: 714 $[M+H]^+$.

Synthesis of 2-(4-methylpiperazin-1-yl)ethanol (12)[24]

Methylpiperazine (3.54 mL, 31.9 mmol, 1.33 eq.) was dissolved in toluene (11 mL), bromoethanol (1.70 mL, 23.9 mmol, 1.00eq.) was slowly added and the mixture was stirred o.n. at r.t. Then it was filtered and the organic phase was recovered, the solvent removed under reduced pressure to give the desired product. Yield: 80%. White solid. ^{1}H-NMR ($CDCl_3$) δ (ppm): 4.51 (s, 1H); 3.14 (m, 2H); 2.01 (m, 10H); 1.78 (s, 3H). ^{13}C-NMR ($CDCl_3$) δ (ppm): 59.8, 58.0, 54.4, 52.6, 45.5. MS (ES) *m/z*: 145 $[M+H]^+$.

Synthesis of 1-(4-methylpiperazin-1-yl)propan-2-ol (13)[30,31]

Methylpiperazine (55.0 µL, 0.50 mmol, 2.00 eq.) was dissolved in toluene (7 mL), 1-bromo-2-propanol (23.0 µL, 0.25 mmol, 1.00eq.) was slowly added and the mixture was stirred o.n. at r.t. Then it was filtered and the organic phase was recovered, the solvent removed under reduced pressure to give the desired product. Yield: 38%. Colourless oil. ^{1}H-NMR (MeOD) δ (ppm): 4.51 (s, 1H); 3.14 (m, 2H); 2.01 (m, 10H); 1.78 (s, 3H). ^{13}C-NMR (MeOD) δ (ppm): 59.8, 58.0, 54.4, 52.6, 45.5. MS (ES) *m/z*: 159.0 $[M+H]^+$.

Synthesis of 1-(4-methylpiperazin-1-yl)butan-2-ol (17)[30,31]

$ZnCl_2$ (12.4 mg, 0.09 mmol, 0.10 eq.) was added to a solution of methylpiperazine (110 µL, 1.00 mmol, 1.10 eq.) and 1,2-epoxybutane (79.0 µL, 0.91 mmol, 1.00 eq.) in ACN (8 mL); the mixture was stirred under reflux 16h. Then purified by flash chromatography using PE:AcOEt:MeOH:Et_3N = 10:8:1:1 as eluent. Yield: 31%. Colourless oil. ^{1}H-NMR ($CDCl_3$) δ (ppm): 3.65-3.59 (m, 1H), 2.47 (m, 8H), 2.34-2.32 (m, 2H), 2.26 (s, 3H), 1.40-1.35 (m, 1H), 0.96-0.91 (m, 3H). ^{13}C-NMR (MeOD) δ (ppm): 71.5, 61.5, 58.2, 57.6, 46.6, 28.3, 9.5. MS (ES) *m/z*: 173.0 $[M+H]^+$.

Synthesis of 2-(4-methylpiperazin-1-yl)-1-phenylethanol (18)[30,31]

Methylpiperazine (125.04 mg, 1.25 mmol), K_2CO_3 (517.60 mg, 3.74 mmol) and styrene-oxide (95.0 µL, 0.83mmol, 1,00 eq) were dissolved in toluene. The reaction mixture was heated at 130°C for

24h. After water was added, the crude was extracted with DCM (X3) and washed with brine. The organic layers were collected, dried over with Na_2SO_4 and the solvent was evaporated under reduced pressure. Then purified by flash chromatography using AcOEt:MeOH= 9:1 as eluent. Yield: 61%. Colourless oil ^{1}H-NMR ($CDCl_3$) δ (ppm): 7.36-7.22 (m, 5H), 4.73-4.70 (m, 1H), 3.69-3.65 (m, 1H), 2.76 (m, 2H), 2.53-2.44 (m, 8H), 2.30 (s, 3H). ^{13}C-NMR ($CDCl_3$) δ (ppm): 142.2, 128.3, 127.5, 125.8, 68.8, 66.2, 55.2, 53.0, 46.0. MS (ES) *m/z*: 221.1 $[M+H]^+$.

Synthesis of 1-(4-methylpiperazin-1-yl)-3-phenylpropan-2-ol (19)

$ZnCl_2$ (14.72 mg, 0.10 mmol, 0.10 eq.) was added to a solution of methylpiperazine (180 µL, 1.62 mmol, 1.50 eq.) and 2-benzyloxirane (142.0 µL, 1.08 mmol, 1.00 eq.) in ACN (8 mL); the mixture was stirred under reflux 12h. Then purified by flash chromatography using DCM:MeOH=95:5.as eluent. Yield: 68%. Colourless oil ^{1}H-NMR ($CDCl_3$) δ (ppm): 7.29-7.19 (m, 5H), 4.02-3.96 (m, 1H), 3.25 (m, 1H), 2.79-2.74 (m, 1H), 2.65-2.61 (m, 3H), 2.37-2.25 (m, 8H), 2.22 (s, 3H). ^{13}C-NMR ($CDCl_3$) δ (ppm): 140.1, 128.3, 127.5, 125.8, 71.1, 65.9, 55.2, 53.0, 46.0, 45.8. MS (ESI) *m/z*: 235.0 $[M+H]^+$.

***In vitro* ADME assays**

Solvents, reagents, NADP, NADPH, D-glucose-6-phosphate, glucose-6-phosphate dehydrogenase and L-α-phosphatidylcoline were purchased from Sigma-Aldrich S.r.l. (Milan, Italy). Brain polar lipid extract (porcine) was purchased from Avanti Polar Lipids, INC (Alabama, USA). Human plasma was obtained from volunteers/donors. Mouse Plasma and MLM were purchased from Sigma-Aldrich S.r.l. (Milan, Italy). HLM pooled male donors (20 mg/mL) were purchased from BD Gentest-Biosciences (San Jose, California). Milli-Q water was used (Millipore, Milford, MA, USA).

UV/HPLC-MS method. LC analyses were performed by Agilent 1100 LC/MSD VL system (G1946C) (Agilent Technologies, Palo Alto, CA) constituted by a vacuum solvent degassing unit, a binary high-pressure gradient pump, an 1100 series UV detector and a 1100 MSD model VL benchtop mass spectrometer was used. The Agilent 1100 series mass spectra detection (MSD) single-

quadrupole instrument was equipped with the orthogonal spray API-ES (Agilent Technologies, Palo Alto, CA). Nitrogen was used as nebulizing and drying gas. The pressure of the nebulizing gas, the flow of the drying gas, the capillary voltage, the fragmentor voltage and the vaporization temperature were set at 40 psi, 9 L/min, 3000 V, 70 V and 350 °C, respectively. UV detection was monitored at 280 nm. The LC-ESI-MS determination was performed by operating the MSD in the positive ion mode. Spectra were acquired over the scan range m/z 50-1500 using a step size of 0.1 u. Chromatographic analysis was performed using a Kinetex EVO C18 100A column (150 x 4.6 mm, 5 µm particle size) at room temperature. Analysis was carried out using a gradient elution of acetonitrile (ACN) and water (H_2O): t = 0min ACN 0%, t = 3min ACN 0%, t = 12min ACN 98%, t =18 min ACN 98%. The analysis was performed at flow rate of 0.6 mL/min and injection volume was 20 µL.

Aqueous Solubility. Each solid compound (1 mg) was added to 1 mL of water. Each sample was mixed at 20 °C, in a shaker water bath for 24 h. The resulting suspension was filtered through a 0.45 µm nylon filter (Acrodisc). The concentration of compound in solution was determined by UV/LC-MS (performed in triplicate) by comparison with the appropriate calibration curve that was obtained from samples of the compound dissolved in methanol at different concentrations.

Stability tests in MeOH, PBS, human and mouse plasma. Each prodrug was dissolved at r.t. in phosphate buffer (12.5 mM, pH 7.4) or methanol up to a final concentration of 100 µM. Aliquot samples (20 µL) were taken at fixed time points (0.25, 0.50, 0.75, 1.0, 2.0, 3.0, 4.0, 5.0, 6.0, 7.0, 8.0, 24.0 and 48 h) and were analyzed by UV/LC-MS.

Both human and mouse plasma (1.5 mL, 55.7 µg protein/mL),[36] phosphate buffer (1.4 mL, pH 7.4, 25 mM) and a solution of prodrug in methanol (100 µL, 3.0 mM) were mixed in a test tube that was incubated at 37 °C. At set time points (0.25, 0.50, 1.0, 2.0, 3.0, 4.0 and 24.0 h), samples of 150 µL were taken, mixed with 600 µL of cold acetonitrile and centrifuged at 5000 rpm for 15 min. The

supernatant was removed and analyzed by UV/LC-MS to monitor the hydrolysis process of prodrug (method reported above).

Parallel Artificial Membrane Permeability Assay (PAMPA). Each 'donor solution' was prepared from a solution of the appropriate compound (DMSO, 1 mM) diluted with phosphate buffer (pH 7.4, 25.0 mM) up to a final concentration of 500 µM. The donor wells were filled with 150 µL of 'donor solution'. The filters were coated with 5 µL of a solution of phosphatidylcholine (in dodecane 1% (w/v) to determine GI permeability) or 4 µL of brain polar lipid solution (20mg/mL, 16% chloroform, 84% dodecane) prepared from chloroform 10% w/v solution (to determine BBB permeability) and filled with 300 µL of 'acceptor solution' (50% v/v DMSO and phosphate buffer). The sandwich plate was assembled and incubated for 5 h at r.t. under gentle shaking. After the incubation time, the sandwich was disassembled and the amount of compound in both the donor and acceptor wells was measured by UV/LC-MS. Permeability (P_{app}) was calculated according to the following equation[37]

$$P_{app} = -\frac{V_D V_A}{(V_D + V_A) A t} \ln(1 - r)$$

where V_A is the volume in the acceptor well (cm^3), V_D is the volume in the donor well (cm^3), A is the "effective area" of the membrane (cm^2), t is the incubation time (s) and r the ratio between drug concentration in the acceptor and equilibrium concentration of the drug in the total volume (V_D+V_A). Drug concentration was estimated by using the peak area integration.

Metabolic Stability in HLM (Human Liver Microsomes) and MLM (Mouse Liver Microsomes). The incubation mixture (total volume of 500 µL) was constituted by the following components: HLM/MLM (0.2 mg/mL, 5 µL), a NADPH regenerating system (NADPH 0.2 mM, $NADPH^+$ 1 mM, D-glucose-6-phosphate 4 mM, 4 unit/mL glucose-6-phosphate dehydrogenase and $MgCl_2$ 48 mM), 50 µM of each compound in DMSO and phosphate buffer (pH 7.4, 25 mM, up to a final volume of 500 µL). The mixture was incubated at 37 °C for 1 h. The reaction was cooled down and quenched with

acetonitrile (1.0 mL). After centrifugation (10^4 rpm, 10 min), the surnatant was taken, dried under nitrogen flow, suspended in 100 µL of methanol and analyzed by UV/LC-MS to determine the percentage of compound that was not metabolized.

Biological Assays

Cellular assays. GBM U87 cells were plated in a 6-well plate (5×10^4 cells per well) in EMEM with 10% FBS, 2 mM L-glutamine, 10000 units/mL Penicillin/Streptomycin and incubated with compounds (DMSO solution) at increasing concentrations (0.1 µM, 1.0 µM, 10 µM and 50 µM) for 24, 48 and 72 h at 37°C in 5% CO_2 atmosphere. Cells were harvested to determine cell amount and viability by Trypan Blue assay. The half maximal inhibitory concentration (IC_{50}) for each compound was estimated fitting a curve with a nonlinear regression created with all the collected data using GraphPad Prism Software, version 6.0.

Cellular Kinetics. GBM U87 cells were seeded in a 6-well plate (3×10^5 cells per well) in triplicate. After 24 h, cells were treated with compound (20 µM) for different periods (0.5, 3.0, 4.0, 7.0, 24 h). Cells were harvested and counted by Trypan Blue assay, cell counts were used for normalization purposes. All the harvested cells were lysed in 150 µL of deionized water, subjected to 10 cycles of freeze and thaw and then sonicated for 10 minute at 560 W (maximum intensity) in a bath sonicator. Standard compound at 10 µM was added in lysed cells as control. Lysed cells were then centrifuged at 5000 × g for 20 minutes and supernatant was withdrawn and dried by nitrogen flow. Samples were resuspended in 100 µL of methanol and the amount of compound within the cells was evaluated by UV/LC-MS analysis.

Human carboxylesterase 1 (hCE 1) assay. Enzymatic hydrolysis of compound **4a** to **4** was examined under the following conditions. Increasing concentrations (10, 50 and 100 µM) of **4a** were incubated with a pre-warmed (37°C) mixture, containing the purified enzyme hCE1 (Purchased from Sigma-Aldrich Milano, Italy) (25 U/reaction) and 50 mM HEPES buffer pH 7.4, for

1 h. All reactions were terminated by addition of equal volume of acetonitrile, and proteins were pelleted by centrifugation for 20 min at 5000 rpm at 4°C. The supernatant from the above reactions were analysed by reverse-phase HPLC-UV-MS, using the gradient method described into the manuscript. Percentage of hydrolysis was determined compared to the control (Fig. S1). All the experiments were conducted in triplicate . All experiments were conducted in triplicate.

***In vivo* PK**

The used animal protocol was reviewed and approved by the animal care and ethics committee of the Università degli Studi di Siena, Italy. Male BALB/C mice (weight 20-30 g) were obtained from Charles River (Milan, Italy). The experiment was performed in triplicate and mice were divided into two groups and treated with drug or prodrug (DMSO solution). The compounds were administered intraperitoneally (100 µL) at the dose of 50 mg/Kg. At several time points (0.25, 0.50, 1.0, 1.5, 2.0, 4.0, 8.0 and 24.0 h), after drug administration, mice were treated i.p. with heparin (5000 U/Kg) and sacrificed under CO_2. Blood and brain were collected for the following quantitative analysis. The blood was centrifuged at 4000 rpm for 20 minutes to separate the plasma fraction, which was subsequently collected in a test tube. Acetonitrile (1 mL, with internal standard at the concentration of 10 µM) was added to each sample to denature proteins. Samples were centrifuged at 4000 rpm for 20 minutes, the supernatant was recovered, dried under vacuum and analyzed. Brain was homogenized using a glass/glass Potter-Elvehjem tissue homogenizer, in order to extract the compound from the tissue, 7 mL of acetonitrile were added (with internal standard at the concentration of 10 µM). Brain samples were then treated as previously described for blood samples. Each brain and blood sample was solubilized in 100 µL of methanol and analyzed by UV/LC-MS. The quantification of each compound was performed by reference to the appropriate calibration curve. PKCALC[30] was used to determine pharmacokinetic parameters.

The used animal protocol for oral administration PK was reviewed and approved by the animal care and ethics committee of the Università degli Studi L'Aquila. Male BALB/C mice (weight 20-30 g) were obtained from Charles River (Milan, Italy). Mice received 50 mg/Kg of **4a** in methylcellulose 0.5% solution per *o.s.* by gavage. At 5 time-points (1, 2, 4, 8 and 24 h) after **4a** administration, mice were sacrificed under CO_2. Blood and brains were collected and analysed as for *i.p.* injection.

***In vivo* orthotopic mouse model**

Male CD1 nude mice (Charles River, Milan, Italy) were maintained under the guidelines established by our Institution (University of L'Aquila), complying with the Italian government regulation for the use of laboratory animals. After anesthetization with 100 mg/Kg ketamine, 15 mg/Kg xylazine, the surgical zone was swabbed with Betadine solution, the eyes coated with Lacri-lube. The head was fixed in a stereotactic frame (mouse stereotaxics instrument, Stoelting Europe, Dublin, Ireland) and a midline scalp incision was made. A small hole was made at 1.0 mm anterior and 2 mm lateral to the exposed bregma. A sterile 5 µL Hamilton syringe with a 26 gauge needle was inserted at a depth of 3.0 mm from the skull surface and withdrawn by 0.5 mm to inject 3×10^3 U-87 cells in a volume of 3 µL. The injection rate was set up to 1 µL/min. The needle was then completely withdrawn from the brain over the course of 4 min (1.0 mm/min), and the skin was sutured. Just before treatment initiation (5 days after injection), animals were randomized to treatment groups of 7 mice each. Compound **4** and its prodrug **4a** were prepared as suspension in 0.5% methylcellulose solution. Each mouse received every other day oral administration of methylcellulose vehicle, 50 mg/Kg of compound **4** or 50 mg/Kg of prodrug **4a**. Mice were euthanized when they displayed neurological signs (e.g. altered gait, tremors/seizures, lethargy) or weight loss of 20% or greater of pre-surgical weight. Data were analyzed through Kaplan-Meier curves considering mean and median survival values (Med Calc software, MedCalc Software bvba,

Ostend, Belgium). The statistical significance was evaluated by the Logrank test and P values <0.05 were considered statistically significant.

SUPPORTING INFORMATION

The supporting information file is available free of charge on the ACS Publication website

[*In vitro* ADME assays methods; enzymatic assays including human carboxylesterase 1 (hCE1) hydrolysis description; NMR spectra of compounds]

CORRESPONDING AUTHOR

E-mail: botta.maurizio@gmail.com

ACKNOWLEDGEMENT

We would like to thank Beatrice Gorelli (Department of Life Science, University of Siena) for the technical support in the pharmacokinetic study.

References

1. Schenone, S.; Radi, M.; Musumeci, F.; Brullo, C.; Botta, M. Biologically driven synthesis of pyrazolo[3,4-*d*]pyrimidines as protein kinase inhibitors: an old scaffold as a new tool for medicinal chemistry and chemical biology studies. *Chem. Rev.* **2014**, *114*, 7189-7238.
2. Yeatman, T.J. A renaissance for SRC. *Nat. Rev. Cancer* **2004**, *4*, 470-480.
3. Spreafico, A.; Schenone, S.; Serchi, T.; Orlandini, M.; Angelucci, A.; Magrini, D.; Bernardini, G.; Collodel, G.; Di Stefano, A.; Tintori, C.; Bologna, M.; Manetti, F.; Botta, M.; Santucci, A. Antiproliferative and proapoptotic activities of new pyrazolo[3,4-*d*]pyrimidine derivative Src kinase inhibitors in human osteosarcoma cells. *FASEB J*. **2008**, *22*, 1560-1571.
4. Angelucci, A.; Schenone, S.; Gravina, G. L.; Muzi, P.; Festuccia, C.; Vicentini, C.; Botta, M.; Bologna, M. Pyrazolo[3,4-*d*]pyrimidines c-Src inhibitors reduce epidermal growth factor-induced migration in prostate cancer cells. *Eur. J. Cancer* **2006**, *42*, 2838–2845.
5. Tintori, C.; Fallacara, A.L.; Radi, M.; Zamperini, C.; Dreassi, E.; Crespan, E.; Maga, G.; Schenone, S.; Musumeci, F.; Brullo, C.; Richters, A.; Gasparrini, F.; Angelucci, A.; Festuccia, C.; Delle Monache, S.; Rauh, D.; Botta, M. Combining X-ray crystallography and molecular modeling toward the optimization of pyrazolo[3,4-*d*]pyrimidines as potent c-Src inhibitors active in vivo against Neuroblastoma. *J. Med. Chem.* **2015**, *58*, 347-361.
6. Navarra, M.; Celano, M.; Maiuolo, J.; Schenone, S.; Botta, M.; Angelucci, A.; Bramanti, P.; Russo, D. Antiproliferative and pro-apoptotic effects afforded by novel Src-kinase inhibitors in human neuroblastoma cells. *BMC Cancer* **2010**, *10*, 602-614.
7. Ceccherini, E.; Indovina, P.; Zamperini, C.; Dreassi, E.; Casini, N.; Cutaia, O.; Forte, I.M.; Pentimalli, F.; Esposito, L.; Polito, M.S.; Schenone, S.; Botta, M.; Giordano, A. SRC family kinase inhibition through a new pyrazolo[3,4-*d*]pyrimidine derivative as a feasible approach for glioblastoma treatment. *J. Cell. Biochem.* **2015**, *116*, 856-863.

8. Calgani, A.; Vignaroli, G.; Zamperini, C.; Coniglio F.; Festuccia, C.; Di Cesare, E.; Gravina, G.L.; Mattei, C.; Vitale, F.; Schenone, S.; Botta M.; Angelucci A. Suppression of SRC signaling is effective in reducing synergy between glioblastoma and stromal cells. *Mol Cancer Ther.* **2016** *15*, 1535-1544.

9. Casini, N.; Forte, I.M., Mastrogiovanni, G.; Pentimalli, F.; Angelucci, A.; Festuccia, C.; Tomei, V.; Ceccherini, E.; Di Marzo, D.; Schenone, S.; Botta, M.; Giordano, A.; Indovina, P. SRC family kinase (SFK) inhibition reduces rhabdomyosarcoma cell growth in vitro and in vivo and triggers p38 MAP kinase-mediated differentiation. *Oncotarget* **2015**, *6*, 12421-12435.

10. Indovina, P.; Giorgi, F.; Rizzo, V.; Khadang, B.; Schenone, S.; Di Marzo, D.; Forte, I.M.; Tomei, V.; Mattioli, E.; D'Urso, V.; Grilli, B.; Botta, M.; Giordano, A.; Pentimalli, F. New pyrazolo[3,4-*d*]pyrimidine SRC inhibitors induce apoptosis in mesothelioma cell lines through p27 nuclear stabilization. *Oncogene* **2012**, *31*, 929-938.

11. Rossi, A.; Schenone, S.; Angelucci, A.; Cozzi, M.; Caracciolo, V.; Pentimalli, F.; Puca, A.; Pucci, B.; La Montagna, R.; Bologna, M.; Botta, M.; Giordano, A. New pyrazolo-[3,4-*d*]-pyrimidine derivative Src kinase inhibitors lead to cell cycle arrest and tumor growth reduction of human medulloblastoma cells. *FASEB J*. **2010**, *24*, 2881-2892.

12. Morisi, R.; Celano, M.; Tosi, E.; Schenone, S.; Navarra, M.; Ferretti, E.; Costante, G.; Durante, C.; Botta, G.; D'Agostino, M.; Brullo, C.; Filetti, S.; Botta. M.; Russo, D. Growth inhibition of medullary thyroid carcinoma cells by pyrazolo-pyrimidine derivates. *J. Endocrinol. Invest.* **2007**, *30*, RC31-34.

13. Radi, M.; Tintori, C.; Musumeci, F.; Brullo, C.; Zamperini, C.; Dreassi, E.; Fallacara, A. L.; Vignaroli, G.; Crespan, E.; Zanoli, S.; Laurenzana, I.; Filippi, I.; Maga, G.; Schenone, S.; Angelucci, A.; Botta, M. Design, synthesis, and biological evaluation of pyrazolo[3,4-*d*]pyrimidines active in vivo on the Bcr-Abl T315I Mutant. *J. Med. Chem.* **2013**, *56*, 5382-5394.

14. Cozzi, M.; Giorgi, F.; Marcelli, E.; Pentimalli, F.; Forte, I.M.; Schenone, S.; D'Urso, V.; De Falco, G.; Botta, M.; Giordano, A.; Indovina, P. Antitumor activity of new pyrazolo[3,4-*d*]pyrimidine SRC kinase inhibitors in Burkitt lymphoma cell lines and its enhancement by WEE1 inhibition. *Cell Cycle*. **2012**, *11*, 1029-1039.

15. Stupp, R.; Mason, WP.; van den Bent, MJ.; Weller, M.; Fisher, B.; Taphoorn, M.J.; Belanger, K.; Brandes, A.A.; Marosi, C.; Bogdahn, U.; Curschmann, J.; Janzer, R.C.; Ludwin, S.K.; Gorlia, T.; Allgeier, A.; Lacombe, D.; Cairncross, J.G.; Eisenhauer, E.; Mirimanoff, R.O. Radiotherapy plus concomitant and adjuvant temozolomide for glioblastoma. *N. Engl. J. Med.* **2005**, *352*, 987-996.

16. Ahluwalia, M.S.; de Groot, J.; Liu, W.M.; Gladson, C.L. Targeting SRC in glioblastoma tumors and brain metastases: rationale and preclinical studies. *Cancer Lett.* **2010**, *298,* 139-149.

17. Dreassi, E.; Zizzari, A. T.; Mori, M.; Filippi, I.; Belfiore, A.; Naldini, A.; Carraro, F.; Santucci, A.; Schenone, S.; Botta, M. 2-Hydroxypropyl-β-cyclodextrin strongly improves water solubility and anti-proliferative activity of pyrazolo[3,4-*d*]pyrimidines Src-Abl dual inhibitors. *Eur. J. Med. Chem.* **2010**, *45*, 5958–5964.

18. Radi, M.; Evensen, L.; Dreassi, E.; Zamperini, C.; Caporicci, M.; Falchi, F.; Musumeci, F.; Schenone, S.; Lorens, J. B.; Botta, M. A combined targeted/phenotypic approach for the identification of new antiangiogenics agents active on a zebrafish model: from in silico screening to cyclodextrin formulation. *Bioorg. Med. Chem. Lett.* **2012**, *22*, 5579-5583.

19. Kerns, E.H.; Di, L. Pharmaceutical profiling in drug discovery. *Drug Discovery Today* **2003**, *8*, 316-323.

20. Di, L.; Kerns, E. H. Profiling drug-like properties in discovery research. *Curr. Op. Chem. Biol.* **2003**, *7*, 402-408.

21. Lipinski, C. A. Drug-like properties and the causes of poor solubility and poor permeability. *J. Pharm. Tox. Methods* **2000**, *44*, 235-249.

22. Vignaroli, G.; Zamperini, C.;Dreassi, E.;Radi, M.;Angelucci, A.;Sanità, P.;Crespan, E.; Kissova, M.; Maga, G.;Schenone, S.;Musumeci, F.;Botta, M. Pyrazolo[3,4-*d*]pyrimidine prodrugs: strategic optimization of the aqueous solubility of dual Src/Abl inhibitors. *ACS Med. Chem. Lett.* **2013**, *4*, 622-626.

23. Vignaroli, G.; Calandro, P.; Zamperini, C.; Coniglio, F.; Iovenitti, G.; Tavanti, M.; Colecchia, D.; Dreassi, E.; Valoti, M.; Schenone, S.; Chiariello, M.; Botta, M. Improvement of pyrazolo[3,4-*d*]pyrimidines pharmacokinetic properties: nanosystem approaches for drug delivery. *Sci. Rep.* **2016**, *6, 21*.

24. Rautio, J.; Kumpulainen, H.; Heimbach, T.; Oliyai, R.; Oh, D.; Järvinen, T.; Savolainen, J. Prodrugs: design and clinical applications. *Nat. Rev.* **2008**, *7*, 255−270.

25. Huttunen, K. M.; Raunio, H.; Rautio, J. Prodrugs-from serendipity to rational design. *Pharmacol. Rev.* **2011**, *63*, 750−771.

26. Schenone, S.; Bruno, O.; Bondavalli, F.; Ranise, A.; Mosti, L.; Menozzi, G.; Fossa, P.; Donnini, S.; Santoro, A.; Ziche, M.; Manetti, F.; Botta, M. Antiproliferative activity of new 1-aryl-4-amino-1*H*-pyrazolo[3,4-*d*]pyrimidine derivatives toward the human epidermoid carcinoma A431 cell line. *Eur. J. Med. Chem*. **2004**, *39*, 939-946.

27. Manetti, F.; Santucci, A.; Locatelli, G.A.; Maga, G.; Spreafico, A.; Serchi, T.; Orlandini, M.; Bernardini, G.; Caradonna, N.P.; Spallarossa, A.; Brullo, C.; Schenone, S.; Bruno, O.; Ranise, A.; Bondavalli, F.; Hoffmann, O.; Bologna, M.; Angelucci, A.; Botta M. Identification of a novel pyrazolo[3,4-*d*]pyrimidine able to inhibit cell proliferation of a human osteogenic sarcoma in vitro and in a xenograft model in mice. *J. Med. Chem.* **2007**, *50*, 5579-5588.

28. Carraro, F.; Naldini, A.; Pucci, A.; Locatelli, G.A.; Maga, G.; Schenone, S.; Bruno, O.; Ranise, A.; Bondavalli, F.; Brullo, C.; Fossa, P.; Menozzi, G.; Mosti, L.; Modugno, M.; Tintori, C.; Manetti, F.; Botta, M. Pyrazolo[3,4-*d*]pyrimidines as potent antiproliferative and proapoptotic agents toward A431 and 8701-BC cells in culture via inhibition of c-Src phosphorylation. *J. Med. Chem.* **2006**, *49*, 1549-1561.

29. Radi, M.; Brullo, C.; Crespan, E.; Tintori, C.; Musumeci, F.; Biava, M.; Schenone, S.; Dreassi, E.; Zamperini, C.; Maga, G.; Pagano, D.; Angelucci, A.; Bologna, M.; Botta, M. Identification of potent c-Src inhibitors strongly affecting the proliferation of human neuroblastoma cells. *Bioorg. Med. Chem. Lett.* **2011**, *21*, 5928-5933.

30. Pinney, K.G.; Miranda, M.G.; Dorsey, J.M. Preparation of piperazine or piperidine derivatives as serotonin reuptake inhibitors acting at both the transporter and receptors. U.S. Pat. Appl. Publ. **2012**/0016124.

31. Botta, M.; Angelucci, A.; Dreassi, E.; Schenone, S.; Tintori, C.; Vignaroli, G. Preparation of 4-amino-substituted pyrazolo[3,4-*d*]pyrimidine and pyrrolo[2,3-*d*]pyrimidine derivative as the Src family kinases. WO 2016066755, June 23, 2016.

32. Ross, M.K.; Crow, J.A. Human carboxylesterases and their role in xenobiotic and endobiotic metabolism. *J. Biochem. Mol. Toxicol.* **2007**, *21*, 187-196.

33. Tintori, C.; Magnani, M.; Schenone, S.; Botta, M. Docking, 3D QSAR studies and in silico ADME prediction on c-Src tyrosine kinase inhibitors. *Eur. J. Med. Chem.* **2009**, *44,* 990-1000.

34. Bjerrum, J.; Schwarzenbach, G.; Sillen, L. G. Stability constants. Part I: Organic ligands; Chemical Society Special Publication No. 6; The Chemical Society: London, U.K., **1957**.

35. Slatter, J.G.; Schaaf, L.J.; Sams, J.P.; Feenstra, K.L.; Johnson, M.G.; Bombart, P.A.; Cathcart, K.S.; Verbug, M.T.; Pearson, L.K.; Compton, L.D.; Miller, L.L.; Baker, D.S.; Pesheck, C.V.; Lord,

R.S. Pharmacokinetics, metabolism, and excretion of irinotecan (CPT-11) following I.V. infusion of [14C]CPT-11 in cancer patients. *Drug Metab. Dispos.* **2000**, *28*, 423−433.

36. Bradford, M.M. A rapid and sensitive method for the quantitation of microgram quantities of protein utilizing the principle of protein-dye binding. *Anal. Biochem.* **1976**, *72*, 248-54.
37. Wohnsland, F.; Faller, B. High-throughput permeability pH profile and high-throughput alkane/water log P with artificial membranes. *J. Med. Chem.* **2001**, *44*, 923-930.

Table Of Contents